PLANT SCIENCE TODAY
Vol 13(sp9): 01-29
https://doi.org/10.14719/pst.16504

eISSN 2348-1900
OPEN ACCESS

Research Article | Agriculture

2026, Volume 13, Issue sp9, pp. 01-29

Validation of satellite precipitation products for multi-timescale drought monitoring in Tamil Nadu, India

Karthika K J D[1], Pazhanivelan S[2*], Sathyamoorthy N K[1], Prabu P C[3], Sivamurugan A P[4] & Vanitha G[5]

[1]Agro Climate Research Centre, Tamil Nadu Agricultural University, Coimbatore 641 003, Tamil Nadu, India
[2]Directorate of Crop Management, Tamil Nadu Agricultural University, Coimbatore 641 003, Tamil Nadu, India
[3]Centre for Water and Geospatial Studies, Tamil Nadu Agricultural University, Coimbatore 641 003, Tamil Nadu, India
[4]Department of Agronomy, Tamil Nadu Agricultural University, Coimbatore 641 003, Tamil Nadu, India
[5]School of Post Graduate Studies, Tamil Nadu Agricultural University, Coimbatore 641 003, Tamil Nadu, Tamil Nadu, India

***Correspondence:** pazhanivelans@tnau.ac.in

Abstract

In monsoon-dominated areas, accurate precipitation data are essential for hydrological modelling, agricultural water management, drought monitoring, flood forecasting and climate adaptation. However, regional validation is required prior to practical use because the accuracy of satellite-based precipitation products (SPPs) varies significantly across different meteorological and physiographic conditions. The performance of three popular SPPs, namely Climate Hazards Center Infrared Precipitation with Stations (CHIRPS), Integrated Multi-satellite Retrievals for Global Precipitation Measurement (IMERG) Final Run and Multi-Source Weighted-Ensemble Precipitation (MSWEP) was assessed in this study using daily rainfall data from 37 synoptic rain gauge stations located throughout Tamil Nadu, India, between 1998 and 2023. Continuous (root mean square error [RMSE], correlation coefficient [CC], percent bias [PBIAS]) and categorical (probability of detection [POD], false alarm ratio [FAR], critical success index [CSI]) metrics, as well as seasonal rainfall assessment and extreme rainfall detection based on India Meteorological Department (IMD) categories, were used to evaluate product performance. The validated precipitation dataset was subsequently used to investigate multi-timescale standardised precipitation index (SPI) analysis from 1991–2023 to examine the progression of drought. The MSWEP performed best, exhibiting the lowest RMSE (11.2 mm), lowest bias (10.0 %), highest correlation (0.30), highest POD (0.753) and highest CSI (0.308), while CHIRPS and IMERG had relatively higher uncertainties, especially in the Western Ghats and cyclone-affected coastal districts. The analysis of multi-timescale SPI detected periods of drought from 2002–2004, 2012–16 and 2018–20, with the North Western, Western and Southern Agro-Climatic zones being the drought-prone areas. The integration of validated MSWEP precipitation data with multi-timescale SPI enhances drought detection and provides a scientific framework for hydrological modelling, irrigation scheduling, drought early warning systems, reservoir management and agricultural planning in Tamil Nadu.

Keywords: CHIRPS; drought; IMERG; MSWEP; satellite-based precipitation products; standardised precipitation index

Received: 02 July 2026. **Accepted:** 01 September 2026. **Published:** 24 November 2026.

Cite this article: Karthika KJD, Pazhanivelan S, Sathyamoorthy NK, Prabu PC, Sivamurugan AP, Vanitha G. Validation of satellite precipitation products for multi-timescale drought monitoring in Tamil Nadu, India. Plant Science Today. 2026;13(sp9):01-29. https://doi.org/10.14719/pst.16504

Introduction

Fluctuations in precipitation and associated climatic variability exert profound impacts on ecological systems, agricultural productivity and socioeconomic stability across monsoon-dominated regions (1, 2). Tamil Nadu, located in the southeastern part of India, is particularly vulnerable due to its strong spatial rainfall gradients driven by diverse physiography and the dual influence of the Southwest and Northeast monsoons. Extreme rainfall events, cyclonic disturbances and prolonged droughts have historically disrupted agricultural output, water resource availability and rural livelihoods (3). Future increases in climate extremes make it crucial to have reliable rainfall information to support adaptation planning and long-term water management (4). Traditional rain gauge networks, though accurate at point locations, remain sparse and unevenly distributed across Tamil Nadu's orographic and coastal belts. This limitation constrains their ability to capture spatiotemporal rainfall variability, particularly in orographically influenced regions such as the Western Ghats and cyclone-prone coastal districts (5, 6). Satellite-based precipitation products (SPPs) are valuable because they offer wide-area, long-term datasets that complement rain-gauge observations. By integrating multi-sensor inputs and advanced bias-correction techniques, SPPs provide enhanced temporal and spatial resolution suitable for hydrological modelling, drought monitoring and flood forecasting (7). Though several studies have examined satellite-based precipitation estimation over India, very few attempts have been made to use multi-timescale drought assessment along with validated precipitation datasets for assessing the drought dynamics across the agro-climatic zones of Tamil Nadu. Rainfall deficit over the long-term influences' groundwater recharge, reservoir storage and

regional water security, whereas precipitation deficit over the short term affects agricultural activities. It is, therefore, important to understand drought dynamics at different time scales.

Among the widely used SPPs, Climate Hazards Center Infrared Precipitation with Stations (CHIRPS), Integrated Multi-satellite Retrievals for Global Precipitation Measurement (IMERG) and Multi-Source Weighted-Ensemble Precipitation (MSWEP) have gained prominence due to their global coverage, fine spatial resolution and long-term continuity (8–10). CHIRPS employs a multi-stage blending approach combining infrared satellite observations, reanalysis data and gauge corrections, making it particularly useful in data-scarce regions (11). The IMERG, developed under National Aeronautics and Space Administration's Global Precipitation Measurement (NASA's GPM) mission, integrates passive microwave and infrared satellite data with gauge observations to provide near-real-time rainfall estimates at high temporal resolution (9, 12). MSWEP adopts a weighted ensemble framework that fuses gauge, satellite and reanalysis inputs, thereby reducing biases and improving representation of rainfall variability (10). Despite these advancements, several studies have shown that the performance of SPPs varies across climatic zones, with degraded accuracy in arid, semi-arid and orographic regions (13).

Tamil Nadu presents a unique challenge for satellite rainfall estimation due to its dependence on the Northeast monsoon, which contributes nearly half of the annual rainfall and its susceptibility to cyclonic events from the Bay of Bengal. Previous evaluations of SPPs across India have reported systematic biases, including overestimation in orographic zones and underestimation during extreme rainfall events (14). In particular, high false alarm ratios and poor detection skill have been observed in semi-arid rain-shadow regions such as western Tamil Nadu, underscoring the need for localised validation (15). Therefore, rigorous assessment of CHIRPS, IMERG and MSWEP against quality-checked gauge observations is essential to quantify their accuracy, biases and event-detection capabilities in this climatically complex state. This study evaluates the performance of CHIRPS, IMERG Final Run and MSWEP against daily rainfall observations from 37 synoptic stations across Tamil Nadu for the period 1998–2023. Using a point-to-point nearest-grid matching approach, ordinary kriging for spatial visualisation and a suite of continuous (root mean square error [RMSE], correlation, percent bias [PBIAS]) and categorical (probability of detection [POD], false alarm ratio [FAR], critical success index [CSI]) metrics, the analysis quantifies both magnitude errors and event-detection skill at daily and seasonal scales. By providing a comprehensive evaluation of three widely used SPPs, this study contributes to the growing body of literature on satellite rainfall validation in monsoon-dominated regions. In addition to evaluating the best performed satellite precipitation products, this study investigates drought dynamics using multi-timescale SPI for drought assessment and climate resilience analysis. These results will offer practical guidance for selecting suitable precipitation datasets for hydrological modelling, drought monitoring, crop insurance design and climate change adaptation in Tamil Nadu. More broadly, the findings underscore the importance of region-specific validation of satellite rainfall products, as no single dataset is universally optimal across diverse climatic and physiographic settings (16).

Materials and Methods

Study area

Tamil Nadu is located in the southeastern part of the Indian peninsula, extending between 8°05′–13°35′ N latitude and 76°15′–80°20′ E longitude and covers an area of approximately 130058 km² (Fig. 1). The state is bounded by the Western Ghats to the west, the Eastern Ghats to the North, the Bay of Bengal to the East and the Indian Ocean to the South, with a coastline of about 1076 km. The physiography is highly diverse, with elevations ranging from sea level along the eastern coastal plains to over 2600 m in the Western Ghats. The Western Ghats form a continuous orographic barrier, while the Eastern Ghats consist of discontinuous hill ranges in the northern part of the state and the interior plateau lies between these systems with elevations between 45 and 150 m, gradually sloping eastward. This pronounced topographic variation strongly controls regional rainfall distribution and hydrological processes. Tamil Nadu experiences a tropical climate, generally hot and humid throughout the year, with mean annual temperatures ranging between 24–32 °C. The climate varies from semi-arid to dry sub-humid and is characterised by two distinct monsoon seasons: the Southwest Monsoon (SWM; June–September) and the Northeast Monsoon (NEM; October–December). The average annual rainfall is approximately 920 mm with substantial spatial variability ranging from less than 700 mm in the western interior rain-shadow regions to more than 1500 mm along the Western Ghats and coastal belts. Unlike most regions of India, Tamil Nadu receives a major share of its rainfall during the NEM, which contributes about 45–50 % of the annual total, while the SWM contributes approximately 32–36 %. Rainfall during the NEM is frequently associated with cyclonic disturbances and depressions over the Bay of Bengal, resulting in high temporal variability and extreme precipitation events, particularly along the coastal districts.

Rain gauge observed data

Rainfall data were obtained from the State Ground and Surface Water Resources Data Centre, Taramani, Chennai which collects and maintains both agrometeorological and hydrometeorological data, enabling coverage even in mountainous regions. The data were carefully and extensively checked for their quality and data availability for the study period from 1998–2023, years with extensive missing data were excluded. Instead of filling the gaps with uncertain results using imputation methods, these years were omitted.

© The Author(s) 2026. Creative Commons CC BY 4.0. Published by Horizon e-Publishing Group.
https://doi.org/10.14719/pst.16504

Consequently, 37 geographical locations as shown in Fig. 1, were selected as the reference ground truth data used to evaluate the performance of the satellite precipitation products as mentioned in Table 1. These stations have been chosen systematically to provide a representation of the diversity of hydroclimatological and physiographical conditions of Tamil Nadu. The network spans areas prone to cyclones like the coastal plains, the orographic regions of the Western Ghats and semi-arid inland areas affected by the rain-shadow effect. Thus, a stratified district sampling approach by considering that each district must consist of one station point has been adopted to ensure that all rainfall regimes and topographic conditions were covered (17, 18).

Satellite-based precipitation products

To assess the reliability of satellite rainfall retrievals, three widely used SPPs - CHIRPS, IMERG Final Run and MSWEP were evaluated against gauge observations. These datasets were selected for the common analysis period of 1998–2023, ensuring temporal consistency across products (Table 2). Each SPP employs distinct estimation algorithms that vary in sensor inputs, data-merging techniques and spatiotemporal resolutions, leading to differences in rainfall representation. Priority was given to products offering long-term continuity and high spatial resolution (0.05°– 0.10°), which are suitable for regional-scale analysis. Daily precipitation data were adopted to maintain compatibility with ground observations, as station records were available only at the daily scale.

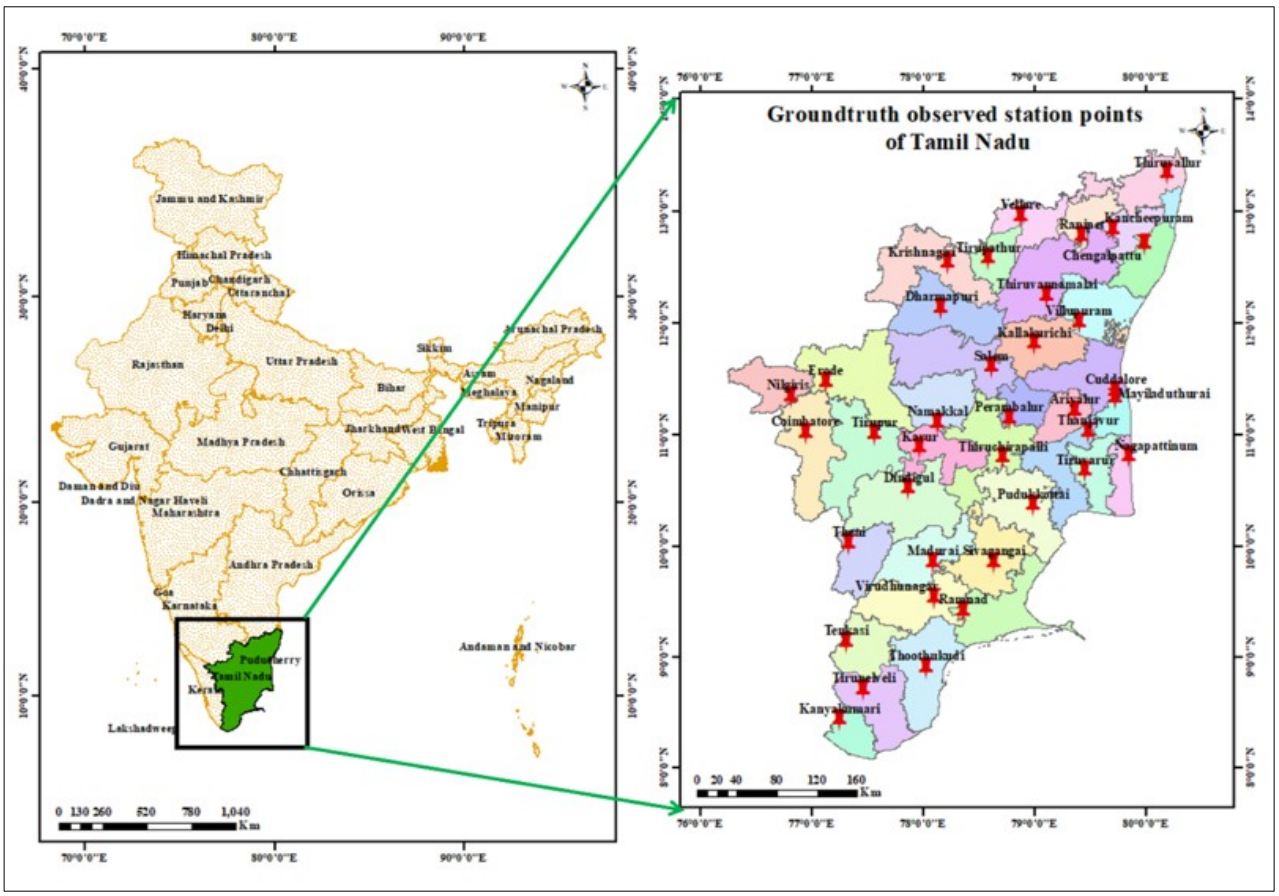


Fig. 1. Geographical locations of ground truth observed station points.

Table 1. Ground truth observed station points of Tamil Nadu for the study

Sl. No	District	Lat	Lon	Sl. No	District	Lat	Lon
1	Ariyalur	11.21	79.36	20	Ramnad	9.41	78.36
2	Chengalpattu	12.7	79.98	21	Ranipet	12.77	79.42
3	Coimbatore	11.01	76.94	22	Salem	11.6	78.61
4	Cuddalore	11.39	79.72	23	Sivagangai	9.85	78.63
5	Dharmapuri	12.13	78.16	24	Tenkasi	9.13	77.31
6	Dindigul	10.51	77.86	25	Thanjavur	11.02	79.48
7	Erode	11.47	77.13	26	Theni	10.02	77.33

© The Author(s) 2026. Creative Commons CC BY 4.0. Published by Horizon e-Publishing Group.
https://doi.org/10.14719/pst.16504

8	Kallakurichi	11.81	78.99	27	Thiruchirapalli	10.79	78.71
9	Kancheepuram	12.83	79.7	28	Thiruvallur	13.33	80.19
10	Kanyakumari	8.43	77.25	29	Thiruvannamalai	12.24	79.11
11	Karur	10.88	77.96	30	Thoothukudi	8.9	78.02
12	Krishnagiri	12.53	78.22	31	Tirunelveli	8.7	77.46
13	Madurai	9.85	78.09	32	Tirupathur	12.57	78.58
14	Mayiladuthurai	11.33	79.72	33	Tirupur	11	77.56
15	Nagapattinum	10.8	79.84	34	Tiruvarur	10.67	79.45
16	Namakkal	11.1	78.13	35	Vellore	12.95	78.87
17	Nilgiris	11.34	76.81	36	Villupuram	12	79.4
18	Perambalur	11.14	78.77	37	Virudhunagar	9.53	78.1
19	Pudukkottai	10.36	78.98				

Table 2. Characteristic features of satellite based precipitation products (SPPs) used in this study

SPP	Spatial coverage	Temporal coverage	Spatial resolution (°)	Temporal resolution (hr)	Institute	Reference
CHIRPS	Land (50° N - 50° S)	1981- near present	0.05°	24	Climate Hazards Centre US Santa Barbara	(8)
IMERG	Global	2000-near present	0.1°	0.5	NASA's Global Precipitation Measurement (GPM) mission	(9)
MSWEP	Global	1979- near present	0.1°	3	GloH2O	(10)

CHIRPS: Climate Hazards Group Infrared Precipitation with Stations; IMERG: Integrated Multi-Satellite Retrievals for Global Precipitation Measurement; MSWEP: Multi-Source Weighted-Ensemble Precipitation.

Climate Hazards Group Infrared Precipitation with Stations

The CHIRPS dataset is a quasi-global gridded rainfall product jointly developed by the United States Geological Survey and the Climate Hazards Group, with support from the United States Agency for International Development (USAID), NASA and National Oceanic and Atmospheric Administration (NOAA). It offers high-resolution precipitation estimates (0.05°, ~5 km) from 1981 to the near present across 50° S–50° N, available at daily, pentadal, decadal and monthly temporal scales (8). CHIRPS is produced through a multi-stage blending approach that combines long-term climatology, infrared satellite observations, satellite-derived rainfall estimates, atmospheric model outputs and extensive ground-based gauge data (5). Rainfall measurements were taken from the nearest CHIRPS grid cell to the corresponding station coordinates. Nearest neighbour matching was chosen over other interpolation (e.g., bilinear interpolation) in order to preserve localised rainfall extremes and avoid artificial smoothing inherent to distance-weighting. Although there is potential for large representativeness errors over sloped terrain, these should be minimal at the high-resolution of the dataset as the distance between the cell points and the actual station location is minimised.

Integrated Multi-Satellite Retrievals for Global Precipitation Measurement

The IMERG precipitation product is developed under the Global Precipitation Measurement (GPM) mission, which succeeded the Tropical Rainfall Measuring Mission. IMERG combines observations from a constellation of passive microwave and infrared satellites, along with ground-based rain gauge data, to produce near-global precipitation estimates (19). IMERG Final Run offers high spatiotemporal resolution rainfall data at 0.1° (~10 km) and 30 min intervals, making it suitable for hydrological and climate applications. Its retrieval framework integrates microwave-based precipitation estimates with infrared observations using advanced morphing and filtering techniques to improve temporal continuity (20). From version V06 onward, reanalysis-based motion vectors enhance precipitation feature tracking and interpolation. Among its outputs, the research-grade Final Run incorporates gauge-based corrections from the Global Precipitation Climatology Centre. The IMERG V06B Final Run provides a consistent long-term rainfall record by merging TRMM- and GPM-era observations and is widely used in validation studies, hydrological modelling and extreme rainfall analysis (9, 12).

Multi-Source Weighted-Ensemble Precipitation

The MSWEP dataset is a global high-resolution rainfall product developed by Hylke Beck, designed to deliver spatially and temporally consistent precipitation estimates through the optimal fusion of multiple data sources. MSWEP version 2 provides fully global coverage at a fine spatial resolution of 0.1° and at 3-hourly, daily and monthly time scales from 1979 to the present (21). It integrates rain gauge observations, several SPPs and atmospheric reanalysis datasets, thereby capitalising on

© The Author(s) 2026. Creative Commons CC BY 4.0. Published by Horizon e-Publishing Group.
https://doi.org/10.14719/pst.16504

the complementary strengths of each source. A weighted ensemble framework is applied, where individual inputs are assigned spatially varying weights based on their performance relative to nearby gauge data. This approach substantially reduces biases and improves representation of precipitation variability, particularly in regions with sparse observations. Compared to its earlier version, MSWEP v2 offers enhanced spatial detail and a better depiction of rainfall extremes. Owing to its robustness and consistency, MSWEP has been widely used in hydrological modelling, water resources assessment and climate variability studies, making it a reliable dataset for comparative precipitation analysis.

Data preprocessing

The preprocessing of these SPPs rainfall datasets involved a systematic workflow that ensures data comparability with rain gauge data (Fig. 2). Raw datasets were acquired in their native formats (NetCDF, HDF5, GeoTIFF) and then converted to a standard format (NetCDF). After that, the datasets were spatially subset to the region of Tamil Nadu and then they were temporally matched with daily rain gauge data, including adjustments for leap years and missing data. Since CHIRPS has a resolution of 0.05° and IMERG and MSWEP have a resolution of 0.10°, resampling was done to harmonize the datasets to a standard grid. For the IMERG data, resampling was done to daily totals, while CHIRPS and MSWEP datasets were used at daily resolution. For each rain gauge, precipitation values were extracted from the nearest grid cell to enable one-to-one comparison. Quality control was done to eliminate negative and unrealistic data and a threshold of 0.5 mm day^{-1} was used to classify rainfall. Contingency tables were used for categorical metrics while continuous metrics were used to quantify magnitude errors.

Evaluation metrics

Independent synoptic rain gauge stations were selected based on their temporal availability of long-term, high-quality rainfall records. The selected rain gauge network was therefore used as reference precipitation for evaluating satellite-derived estimates. Validation was conducted using a point-to-point comparison approach, in which observed rainfall at each station was matched with precipitation values extracted from the nearest grid cell of each satellite product. This approach ensured that the original satellite retrievals were preserved and is widely adopted in remote sensing evaluation studies. Because rain gauge observations represent spatially discrete measurements, spatial interpolation was performed to generate continuous rainfall surfaces. Ordinary kriging was applied due to its ability to account for spatial autocorrelation and to minimise estimation errors. Interpolated rainfall maps were utilised for spatial analysis and visualisation.

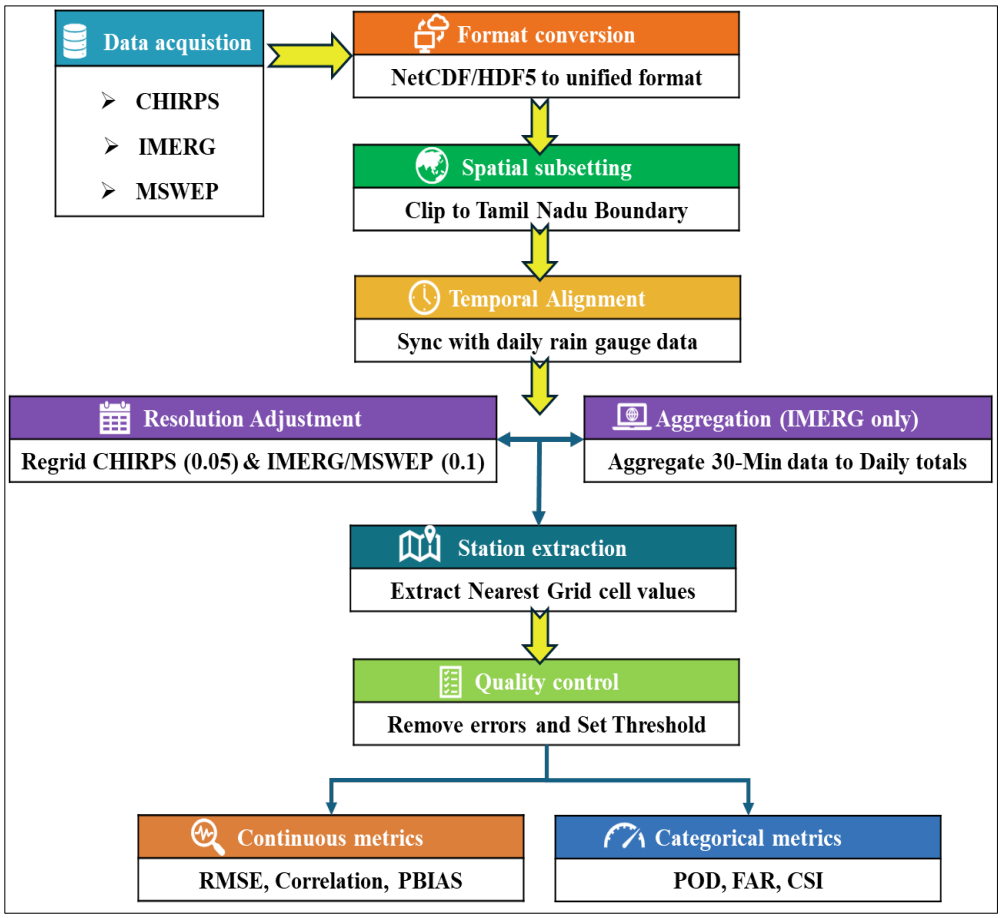


Fig. 2. Flowchart for data preprocessing steps for satellite-based precipitation products (SPPs).

© The Author(s) 2026. Creative Commons CC BY 4.0. Published by Horizon e-Publishing Group.
https://doi.org/10.14719/pst.16504

Product performance was evaluated using both continuous and categorical statistical metrics, providing complementary insights into precipitation estimation accuracy. Continuous metrics were employed to quantify the agreement between satellite-derived and observed rainfall amounts, while categorical metrics were used to assess rainfall occurrence detection. Three continuous and three categorical indices were computed to evaluate the capability of each product in reproducing rainfall magnitude and event occurrence across temporal scales. All spatial analyses and mapping were performed using ArcGIS 10.8 version.

Continuous statistical metrics

Three commonly used statistical measures were applied to quantitatively evaluate the performance of the satellite rainfall products (10, 22). Well-established continuous metrics, including the Pearson correlation coefficient (CC) and RMSE, were calculated at each grid point across the study area for the entire study period. In addition, both systematic and random errors present in the satellite-derived precipitation estimates were examined using an error decomposition approach (23). Understanding these error components is important for both data developers and users, as it helps to identify the sources of uncertainty in the products. To assess overall accuracy, several performance metrics namely the RMSE, CC and percent bias (PBIAS) were used to evaluate how well the satellite products reproduced the observed rainfall amounts and their variability as represented in Table 3.

RMSE represents the average difference between satellite-estimated rainfall and ground-based observations. It shows how large the errors are, on average, between the two datasets (24, 25). Pearson's correlation coefficient is a unitless measure that shows how closely the satellite-estimated rainfall matches the rainfall observed at ground stations (26). PBIAS is used to quantify the systematic deviation between satellite-estimated rainfall and rain gauge observations by expressing the average error as a percentage of the observed rainfall (27).

Categorical metrics

Categorical metrics were used to evaluate the ability of SPPs to detect rainfall events. Three indices - POD, FAR and CSI were calculated using a 2 × 2 contingency table constructed from satellite estimates and gauge observations. The computation of categorical performance metrics begins with the construction of a contingency table based on the comparison between SPP and observed station data as mentioned in Table 4. This table consists of four fundamental elements: hits, misses, false alarms and correct negatives.

A hit (H) occurs when both the satellite product and the rain gauge record a precipitation event, whereas a correct negative is identified when both sources indicate no rainfall. In contrast, a miss (M) represents an observed rainfall event that is not detected by the satellite product, while a false alarm (F) corresponds to rainfall detected by the satellite but not confirmed by ground observations. The categorical indices were evaluated at the daily scale using threshold-based classification of precipitation events as explained in Table 5. A commonly adopted threshold of 0.5 mm day^{-1} was applied to reduce uncertainties associated with light rainfall (23, 28, 29). These metrics assess rainfall occurrence rather than magnitude and range from 0–1.

Probability of detection quantifies the ability of SPPs to correctly identify rainfall events observed by rain gauges (30). It represents the fraction of observed precipitation occurrences that are successfully detected by the satellite estimates. The FAR is used to assess the reliability of SPPs by quantifying how often rainfall is detected when no precipitation is observed by ground stations (31, 32). It represents the proportion of satellite-detected rainfall events that are not confirmed by gauge observations (30). The CSI also referred to as the threat score, provides an overall measure of a product's ability to correctly detect precipitation events (31, 33). It represents the proportion of rainfall occurrences that are simultaneously observed by rain gauges and correctly identified by SPPs (34).

Table 3. Continuous metrics used for validation of satellite based precipitation products (SPPs)

Metrics	Formula	Range	Perfect score	Interpretation
RMSE	$\sqrt{\frac{1}{n}\sum_{i=1}^{n}(S_i - O_i)^2}$	0 to ∞	0	Lower RMSE indicates better agreement whereas higher values indicate greater variability
CC	$\frac{\sum_{i=1}^{n}(O_i - \bar{O})(S_i - \bar{S})}{\sqrt{\sum_{i=1}^{n}(O_i - \bar{O})^2}\sqrt{\sum_{i=1}^{n}(S_i - \bar{S})^2}}$	-1 to +1	1	Higher CC indicates stronger relationship with observed data
PBIAS	$\frac{\sum_{i=1}^{n}(S_i - O_i)}{\sum_{i=1}^{n}(O_i)} \times 100$	-∞ to +∞	0	Positive PBIAS tends to overestimate rainfall whereas negative values indicate underestimation

S: satellite product; O: observed station data; RMSE: root mean square error; CC: Pearsons correlation coefficient; PBIAS: percent bias.

© The Author(s) 2026. Creative Commons CC BY 4.0. Published by Horizon e-Publishing Group.
https://doi.org/10.14719/pst.16504

Table 4. Contingency table for satellite based precipitation products (SPPs) predicted and observed data

SPP (estimated data)	Station (Observed data)		Total
	Yes	No	
Yes	Hit	False alarm	Estimated Yes
No	Miss	Correct negative	Estimated No
Total	Observed Yes	Observed No	

Table 5. Categorical metrics used for validation of satellite based precipitation products (SPPs)

Metrics	Formula	Range	Perfect score	Interpretation
POD	$\frac{H}{H + M}$	0–1	1	Higher values indicate a greater ability to correctly detect rainfall events
FAR	$\frac{F}{H + F}$	0–1	0	Lower values indicate fewer false rainfall detections and better reliability
CSI	$\frac{H}{H + M + F}$	0–1	1	Higher values reflect better overall rainfall detection skill

POD: probability of detection; FAR: false alarm ratio; CSI: critical success index.

Statistically significant testing

Although the validation metrics can depict the magnitude of the differences among the satellite products, they cannot indicate whether the differences are statistically significant. The non-parametric Wilcoxon signed-rank test (34) was thus used for each of the metric (RMSE, CC, PBIAS, POD, FAR, CSI) on the paired station values in each of the product pairs (CHIRPS/IMERG, CHIRPS/MSWEP, IMERG/MSWEP), since this test is appropriate for paired non-normal datasets, such as station precipitation estimates (33). Because three paired tests were conducted for each metric, the significance threshold was adjusted using the Bonferroni correction procedure (35). Specifically, the *p*-value threshold was set to 0.05 for each paired test, meaning that each metric was considered significantly difference between two products if the probability of obtaining the observed result was lower than 5 % (adjusted *p*-value). The test was carried out separately for the daily and seasonal aggregated values.

Standardised precipitation index analysis

With the help of long-term monthly precipitation data, the frequency, duration, magnitude and intensity of meteorological droughts in Tamil Nadu were determined using the SPI. The SPI values were derived through fitting the historical data set for precipitation at each location to a gamma probability distribution, which in turn was transformed to a normal distribution with zero mean and one standard deviation. In this way, different geographical locations having different precipitation patterns can be compared concerning their drought situation. As per the conventional criteria proposed the SPI values were estimated at the accumulation period representing short-term (1–3 months), medium-term (6–12 months) and long-term (24–48 months) drought severity classification as given in Table 6 (35). A drought event was considered to begin when SPI values continuously decreased to ≤ −1.0 and ended when the index became positive. Short-term SPI reflects meteorological anomalies and agricultural drought impacts, medium-term SPI highlights seasonal water stress and hydrological deficits, while long-term SPI identifies multi-year drought cycles and cumulative hydrological stress (36). The computed SPI series at multiple temporal scales were subsequently used to characterise drought evolution, persistence and recurrence over Tamil Nadu, thereby providing a standardised basis for spatial and temporal drought assessment. The SPI analysis was based exclusively on the best performed validated precipitation dataset, the residual uncertainty as estimated from the results was taken into consideration when interpreting the drought classifications. The best performed product is likely to have a small systematic error, which could have affected the SPI calculations near the decision thresholds. SPI values were calculated using the formula:

$$SPI_i = \frac{Xi - Xmean}{\sigma}$$

Where:

X_i = rainfall of station for period *i*

X_{mean} = long-term mean rainfall

σ = standard deviation of rainfall for the same period

Table 6. Standardised precipitation index (SPI)-based drought intensity classification

SPI values	Intensity
>2.00	Extremely wet
1.50–1.99	Very wet
1.00–1.49	Moderate wet
-0.99–+0.99	Near normal
-1.49–-1.00	Moderate drought
-1.99–-1.50	Severe drought
< -2.00	Extremely drought

By applying SPI across multiple timescales, the study captured high-frequency fluctuations, seasonal drought persistence and long-term drought memory. This multi-scale approach provided insights into drought onset, propagation and recovery phases, complementing rainfall deviation analysis. Together, these methods established a comprehensive framework for monitoring rainfall variability and drought dynamics for Tamil Nadu, supporting agricultural planning, water resource management and climate resilience strategies in semi-arid regions.

Extreme rainfall event analysis

Extreme rainfall events were assessed using the Indian Meteorological Department (IMD) classification of 24 hr accumulated rainfalls in terms of intensity levels with seven categories (Standard operating procedure–weather forecasting and warning, 2021). The threshold for all the categories was recently updated and can be

© The Author(s) 2026. Creative Commons CC BY 4.0. Published by Horizon e-Publishing Group.
https://doi.org/10.14719/pst.16504

found in Table 7. Daily rainfall data from 37 synoptic stations of Tamil Nadu (1998–2023) were selected to obtain the frequency of occurrence and distribution of such rainfall to distinguish rainfall caused by monsoon from rainfall caused by cyclones. Subsequently, SPPs were selected corresponding to the same date and district and categorical performance indicators (POD, FAR, CSI) were calculated to see how well SPPs detect IMD classified rainfall. Heatmaps were created to visualise differences in the capability of rainfall detection and occurrence. The proposed approach complies with the current approaches in validating extreme rainfall events using IMD thresholds in satellite rainfall detection during monsoon and convective extremes (14, 15, 23, 37).

Table 7. Indian Meteorological Department (IMD) classification on heavy rainfall events

Category	Range of daily rainfall (mm)
Very light rain	Trace – 2.4 mm
Light rain	2.5 – 15.5 mm
Moderate rain	15.6 – 64.4 mm
Heavy rain	64.5 – 115.5 mm
Very heavy rain	115.6 – 204.4 mm
Extremely heavy rain	>204.5 mm
Exceptionally heavy rain	Actual rainfall amount exceeds 240 mm.

Results

Performance assessment of daily precipitation estimates

Statistical evaluation

The evaluation of SPP is a critical step in ensuring their applicability for hydrological modelling and climate impact studies, particularly in regions characterised by complex climatic regimes such as Tamil Nadu, India. In this study, three widely utilised SPPs such as CHIRPS, IMERG and MSWEP were assessed at the daily time scale using a suite of statistical performance metrics each providing complementary insights into the accuracy and reliability of rainfall detection (Table 8).

Table 8. Performance assessment of CHIRPS, IMERG and MSWEP at daily time scale

SPPs (Mean)	RMSE (mm)	Correlation	PBIAS (%)	POD	FAR	CSI
CHIRPS	11.5	0.29	25.3	0.579	0.681	0.257
IMERG	12.0	0.27	20.5	0.662	0.664	0.286
MSWEP	11.2	0.30	10.0	0.753	0.656	0.308

POD: probability of detection; FAR: false alarm ratio; CSI: critical success index; CHIRPS: Climate Hazards Group Infrared Precipitation with Stations; IMERG: Integrated Multi-Satellite Retrievals for Global Precipitation Measurement; MSWEP: Multi-Source Weighted-Ensemble Precipitation.

Among the three, MSWEP performed best, as it yielded the lowest RMSE (11.2 mm), the highest correlation (0.30), the lowest bias (10.0 %), the highest POD (0.753), the lowest FAR (0.656) and the highest CSI (0.308), which indicates the best accuracy in detecting and estimating rainfall amounts. While CHIRPS has the worst performance in detecting rainfall, as it has the lowest POD (0.579) and the highest FAR (0.681) along with the highest positive bias of 25.3 %. The performance of the IMERG product was moderate with a POD of 0.662 and a positive bias of 20.5 % showing a clear overestimation trend. Thus, from the table, for the estimation and detection of daily rainfall, the best product to use for such a region with complex climatic conditions is the MSWEP product.

The distribution and variability of evaluation metrics were represented in Fig. 3, as box plots for each SPPs revealed distinct differences with confidence intervals (95 % CI) providing a quantitative measure of uncertainty. The range of the RMSE was found to vary from 8–18 mm, with the median being near 12 mm for all products. CHIRPS exhibited a mean RMSE of 11.5 mm (CI: 10.7–12.2 mm), IMERG 12.0 mm (11.3–12.7 mm), while MSWEP achieved the lowest RMSE of 11.2 mm with the tightest interval (10.5–11.9 mm), confirming its superior accuracy. The correlation coefficient ranged from near zero to ~0.45 in which MSWEP resulted maximum correlation coefficient with a median of 0.30 (CI: 0.28–0.33) where the narrower CI for MSWEP demonstrated statistical robustness, followed by CHIRPS with 0.29 (CI: 0.26–0.32) and IMERG with 0.27 (CI: 0.25–0.30). PBIAS values were found to have systematic overestimation for IMERG and CHIRPS with values ranging up from + 20.5 % (CI: 12.6–29.7 %) and + 25.3 % (CI: 16.0–37.9 %). On the other hand, MSWEP had lower bias ranged from + 5 to + 15 % (CI: 2.9–18.7 %) underscoring its resilience against retrieval errors. For detection events, POD ranged from 0.55–0.80. MSWEP had the maximum POD of 0.753 (CI: 0.74–0.76), followed by IMERG with 0.66 (CI: 0.65–0.67) and CHIRPS with 0.58 (CI: 0.56–0.59). FAR ranged from 0.60–0.70. Although CHIRPS (0.681; CI: 0.66–0.70) and IMERG (0.664; CI: 0.64–0.68) had higher FAR, MSWEP had slightly lower FAR at 0.65 (CI: 0.64–0.68). Meanwhile, CSI ranged from 0.20–0.35. In which MSWEP had the maximum CSI (CI: 0.29–0.32), followed by IMERG with 0.29 (CI: 0.27–0.30) and CHIRPS with 0.26 (CI: 0.25–0.27). A smaller width of confidence intervals for all the considered metrics suggests that the performance of the MSWEP product is robust and statistically reliable in the different physiographic zones, while larger confidence intervals for CHIRPS and IMERG products demonstrate the sensitivity of the products to the terrain complexity and cyclone-prone zones.

Pairwise Wilcoxon signed-rank tests were performed by using the Bonferroni correction on the station-level values (n = 37) for each of the performance metrics (Table 9). For the continuous accuracy metrics RMSE and CC, MSWEP was found to perform significantly better than IMERG (n = 37) but not significantly different than CHIRPS ($p < 0.001$ and $p = 0.079$), an indication that while MSWEP had a slightly lower mean RMSE as well as higher CC than CHIRPS, these differences were not significant at the $p = 0.064$ level.

© The Author(s) 2026. Creative Commons CC BY 4.0. Published by Horizon e-Publishing Group.
https://doi.org/10.14719/pst.16504

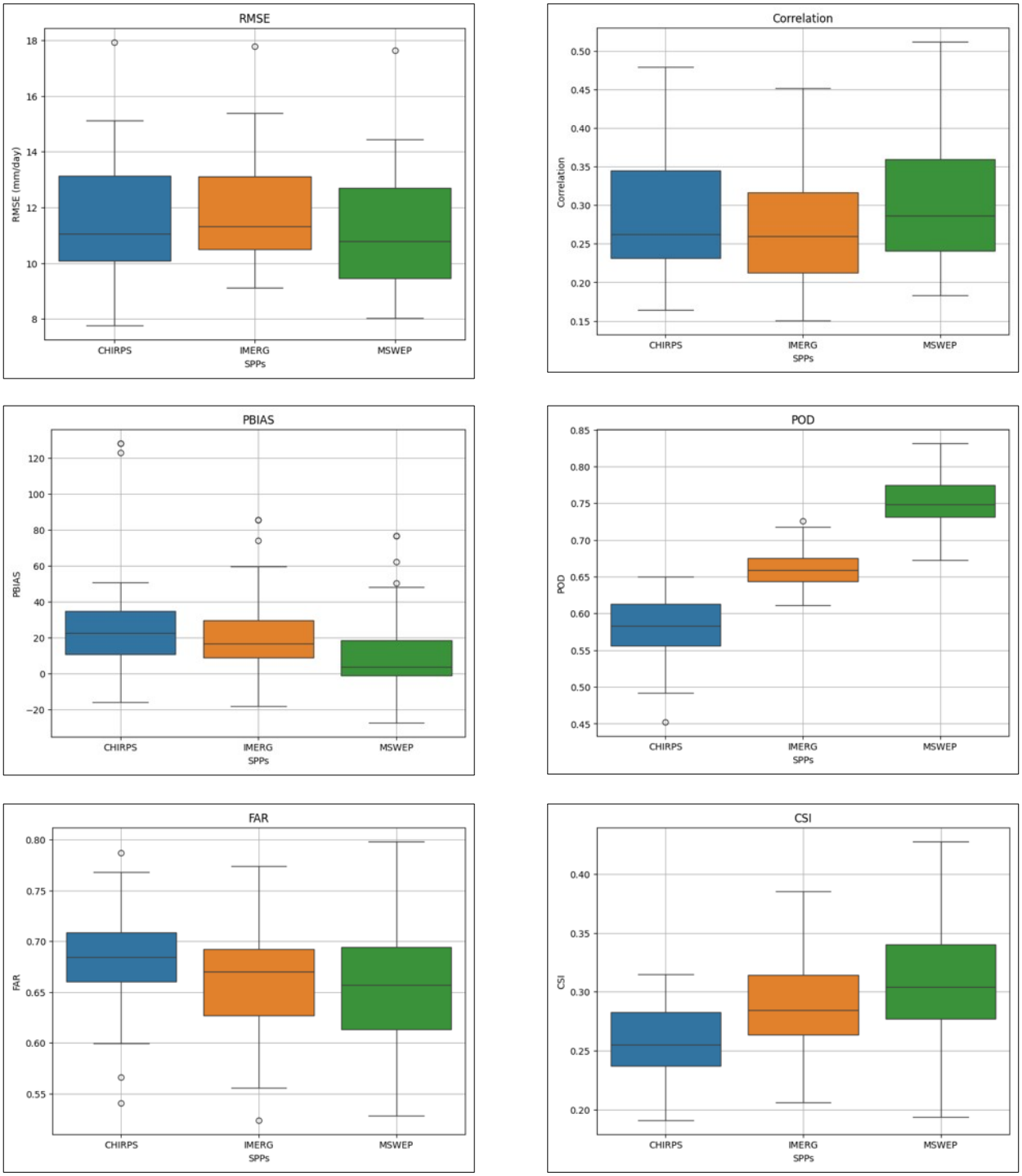


Fig. 3. Box plots of accuracy and detection metrics of satellite-based precipitation products (SPPs).

Table 9. Pairwise Wilcoxon signed-rank test results at daily scale

Metric	Comparison	W statistic	p (Bonferroni)	Significance
RMSE	CHIRPS vs IMERG	127.0	0.0013	*
RMSE	CHIRPS vs MSWEP	205.0	0.0792	ns
RMSE	IMERG vs MSWEP	1.0	<0.001	**
CC	CHIRPS vs IMERG	165.0	0.0124	*
CC	CHIRPS vs MSWEP	200.0	0.0644	ns
CC	IMERG vs MSWEP	0.0	<0.001	**
PBIAS	CHIRPS vs IMERG	254.0	0.1731	ns

© The Author(s) 2026. Creative Commons CC BY 4.0. Published by Horizon e-Publishing Group.
https://doi.org/10.14719/pst.16504

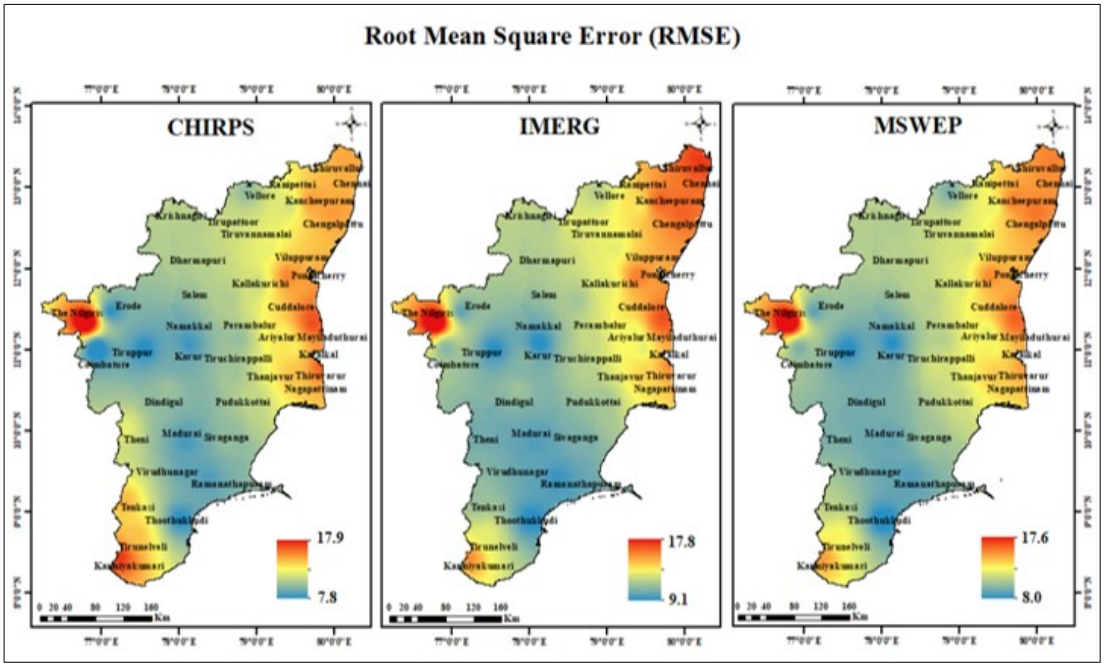
PBIAS	CHIRPS vs MSWEP	81.0	<0.001	**
PBIAS	IMERG vs MSWEP	84.0	0.0001	**
POD	CHIRPS vs IMERG	0.0	<0.001	**
POD	CHIRPS vs MSWEP	0.0	<0.001	**
POD	IMERG vs MSWEP	0.0	<0.001	**
FAR	CHIRPS vs IMERG	66.0	<0.001	**
FAR	CHIRPS vs MSWEP	76.0	<0.001	**
FAR	IMERG vs MSWEP	189.0	0.0399	*
CSI	CHIRPS vs IMERG	7.0	<0.001	**
CSI	CHIRPS vs MSWEP	6.0	<0.001	**
CSI	IMERG vs MSWEP	16.0	<0.001	**

ns: not significant ($p \geq 0.05$); * $p < 0.05$; ** $p < 0.01$; p-values are Bonferroni-corrected for three pairwise comparisons per metric (n = 37 stations); POD: probability of detection; FAR: false alarm ratio; CSI: critical success index; CHIRPS: Climate Hazards Group Infrared Precipitation with Stations; IMERG: Integrated Multi-Satellite Retrievals for Global Precipitation Measurement; MSWEP: Multi-Source Weighted-Ensemble Precipitation.

In the case of the categorical detection metrics, MSWEP had significantly higher skill than both CHIRPS and IMERG in all three metrics (POD, FAR and CSI; $p < 0.01$ for all), an indication that its generally better performance in terms of event detection was not due to chance. For the PBIAS, MSWEP had significantly lower bias than CHIRPS ($p < 0.001$) as well as IMERG ($p < 0.001$), while the latter two products did not differ significantly from each other ($p = 0.173$), an indication that while both infrared and microwave-based products tend to overestimate rainfall amounts relative to rain gauges in a similar manner, the ensemble approach of MSWEP has lower systematic error.

Spatial variability

Spatial analysis further highlights the heterogeneity in product accuracy across physiographic zones of Tamil Nadu. For spatially distributed continuous metrics as shown in Fig. 4 illustrates that higher RMSE values were concentrated along the eastern coastal belt and the Western Ghats, areas strongly influenced by cyclonic rainfall, complex terrain and orographic lifting, which complicate satellite rainfall estimation. Correlation values were generally lower in western ghats, while positive PBIAS patterns confirmed the tendency of CHIRPS and IMERG to overestimate rainfall. In contrast, MSWEP demonstrated relatively better performance across these challenging zones, suggesting that satellite input offers resilience against retrieval errors in areas dominated by extreme rainfall and rough topography.



© The Author(s) 2026. Creative Commons CC BY 4.0. Published by Horizon e-Publishing Group.
https://doi.org/10.14719/pst.16504

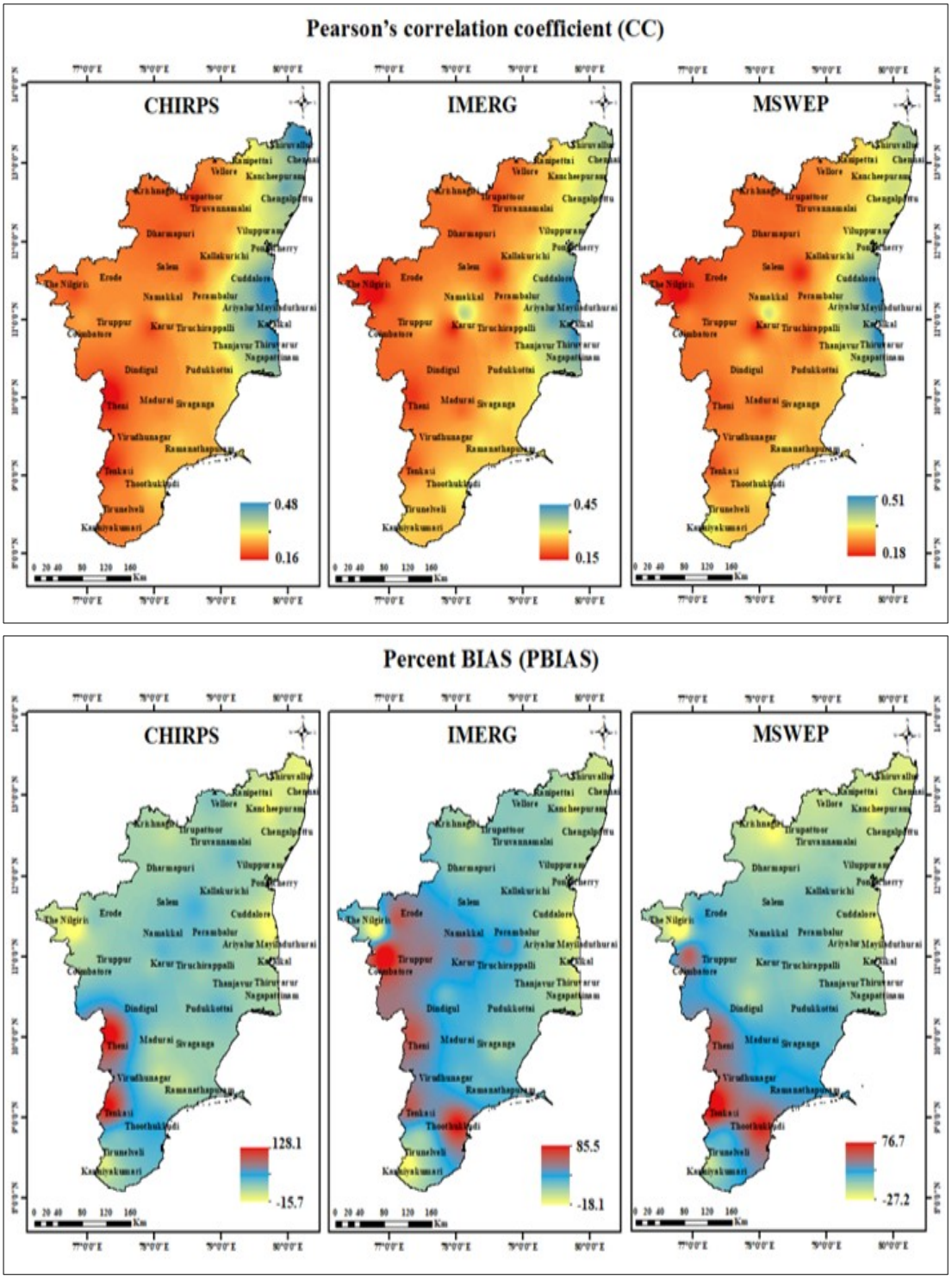


Fig. 4. Spatial distribution of accuracy metrics (root mean square error [RMSE], correlation and percent bias [PBIAS]) for daily precipitation estimates of satellite-based precipitation products (SPPs).

Spatial distribution analysis of categorical detection metrics (Fig. 5) reveals distinct regional patterns in the performance of CHIRPS, IMERG and MSWEP across Tamil Nadu. The POD spatially resulted that MSWEP consistently achieving higher values (0.672–0.872), particularly in southern and coastal districts, while IMERG displayed moderate skill (0.611–0.726) and CHIRPS lower values (0.452–0.650), indicating more missed events. The FAR revealed higher false alarms for CHIRPS and IMERG in central and coastal zones (0.540–0.787 and 0.524–0.774), whereas MSWEP maintained lower and more stable values (0.528–0.798), reflecting better discrimination of rainfall events. The CSI further confirmed MSWEP's superior detection accuracy (0.194–0.428), especially in southern and orographically influenced regions, while IMERG showed moderate CSI (0.208–0.385) and CHIRPS lower values (0.191–0.315), particularly in central Tamil Nadu, underscoring MSWEP's overall reliability.

© The Author(s) 2026. Creative Commons CC BY 4.0. Published by Horizon e-Publishing Group.
https://doi.org/10.14719/pst.16504

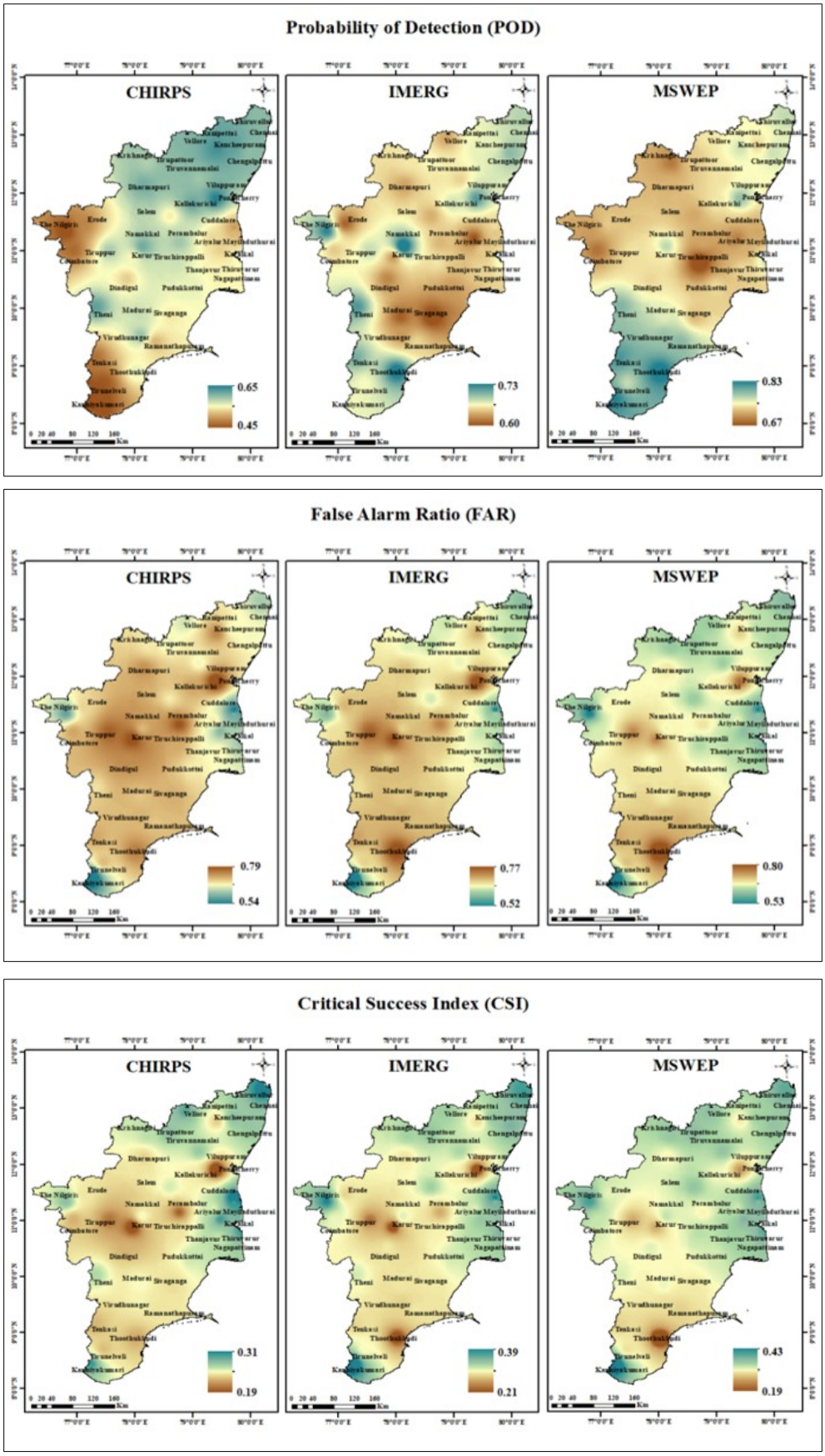


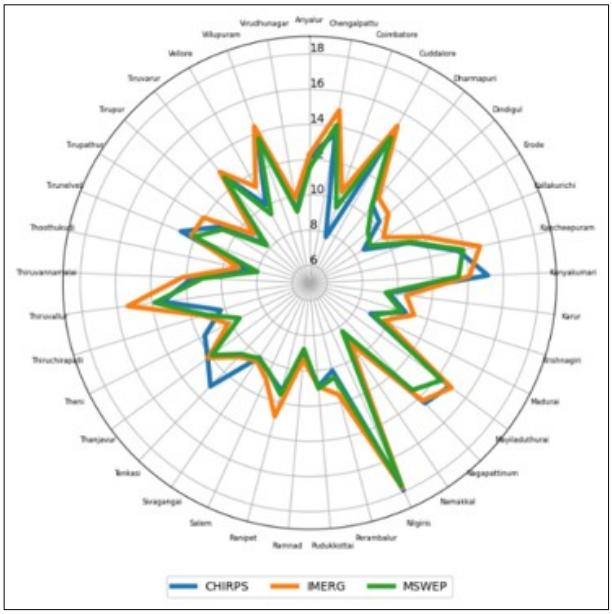
Fig. 5. Spatial distribution of detection metrics (probability of detection [POD], false alarm ratio [FAR], critical success index [CSI]) for daily precipitation estimates of satellite-based precipitation products (SPPs).

© The Author(s) 2026. Creative Commons CC BY 4.0. Published by Horizon e-Publishing Group.
https://doi.org/10.14719/pst.16504

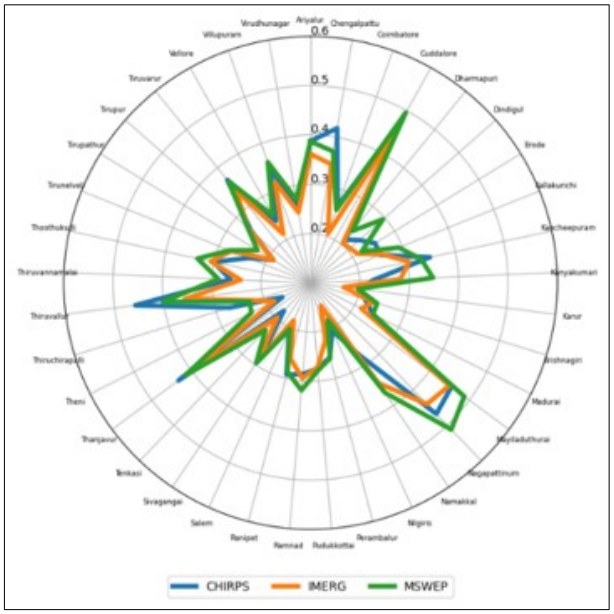
Station-level variability

For the purpose of spatial reliability assessment of SPPs, especially in regions of varied topography and climatic gradients, radar chart diagnostics are useful for evaluating different SPPs based on their performance metrics. Variability in the performance of different SPPs at various stations in terms of different parameters like RMSE, correlation, PBIAS, POD, FAR and CSI is shown in Fig. 6, which clearly indicates the spatial heterogeneity in the study area. The range of RMSE varies between 5 and 35 mm day^{-1}. At stations such as Coimbatore, Erode and Karur, lower errors are found compared to those at stations such as Nilgiris, Salem and Dharmapuri. The correlation values varied between 0.30 and 0.85. Better performance was found at stations such as Tirupur, Madurai and Dindigul compared to stations such as Nilgiris and Krishnagiri. The PBIAS varies between -60 and +80 %, showing both underestimation and overestimation at different stations. Underestimation occurs at stations such as Nilgiris and Theni, while overestimation occurs at stations such as Salem and Vellore.

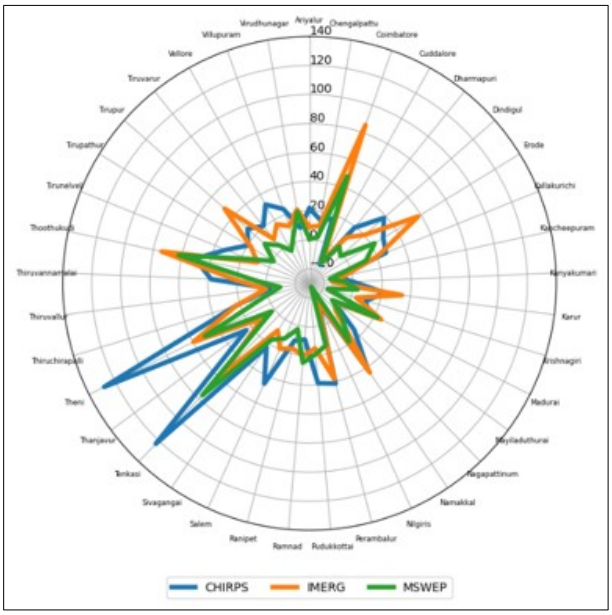
RMSE



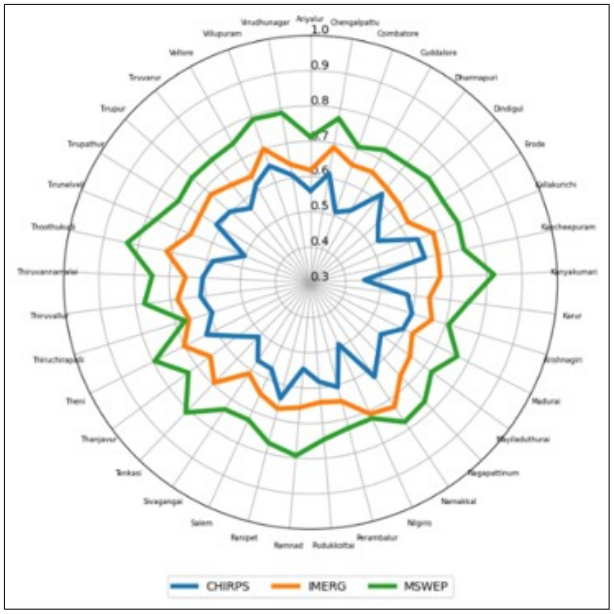
Correlation



PBIAS



POD



© The Author(s) 2026. Creative Commons CC BY 4.0. Published by Horizon e-Publishing Group.
https://doi.org/10.14719/pst.16504

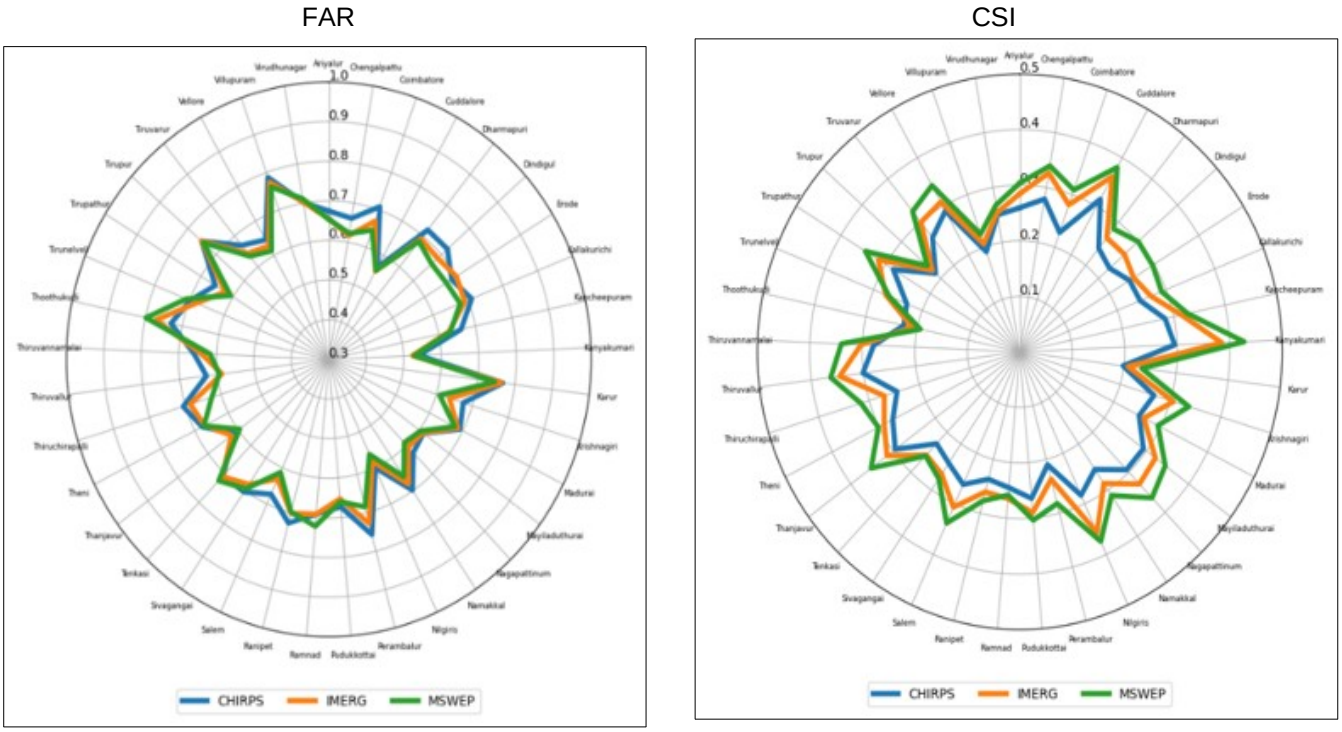


Fig. 6. Station-wise radar chart comparison of evaluation metrics for satellite-based precipitation products (SPPs).

For detection metrics, POD ranges from 0.4–0.85 showing better rainfall detection in the case of Madurai, Tirunelveli and Ramanathapuram, while low detection was observed in Nilgiris and Dharmapuri. The FAR values (0.2–0.6) indicated lower false alarm rate for Coimbatore and Erode, while a high false alarm rate was recorded in Salem and Krishnagiri. The CSI, which encompasses hits, misses and false alarm rates, ranges from 0.3–0.7. This shows a high value in the case of Tirupur, Madurai and Karur, while a low value is recorded in the case of Nilgiris and Dharmapuri.

Extreme rainfall event validation

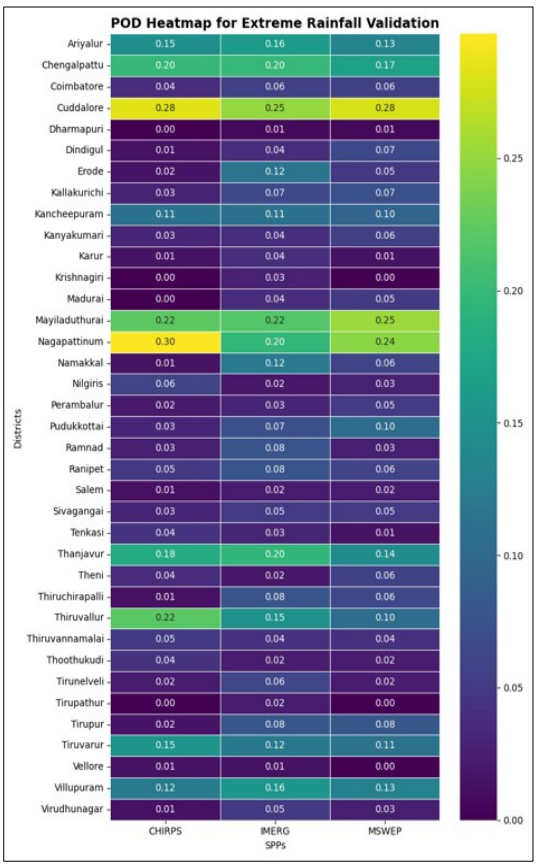
As part of the analysis of detecting high rainfall events based on IMD classification, Fig. 7 illustrates the observed point rainfall intensity across Tamil Nadu, organised into three categories of heavy, very heavy and extreme rainfall days. Cuddalore, Nagapattinam, Mayiladuthurai, Thiruvarur, Villupuram and the Nilgiris ranked highest among all three classifications. These districts were consistent with their coastal or deltaic exposure to Bay of Bengal depression tracks during the NEM, along with orographic lifting in the case of the Nilgiris. On the other hand, interior districts like Dindigul, Erode, Karur, Krishnagiri, Madurai, Perambalur and Virudhunagar showed less exposure to this monsoon and remained low throughout all severity levels. The spatial variation of the extreme rainfall days was more prominent than that of the heavy and very heavy rainfall events. Most of the districts had no days of extreme rainfall or had a few isolated occurrences. However, districts like Cuddalore, Nilgiris, Kallakurichi, Nagapattinam, Namakkal and Thiruvallur had relatively higher occurrences all along. These districts are found in all rainfall intensity categories, indicating their tendency towards intense precipitation events. The pattern is likely to be associated with the combined effect of proximity to the coast, frequent passing of monsoon depressions and cyclonic systems and orographic effects of the surrounding terrain.

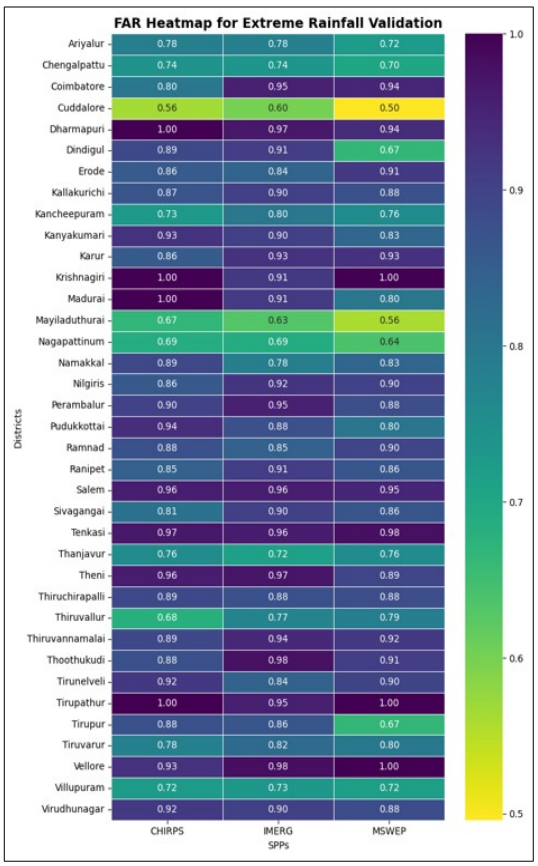
The heatmap-based extreme rainfall event validation using categorical metrics revealed considerable spatial variability in the performance of CHIRPS, IMERG and MSWEP across Tamil Nadu during 1998–2023 (Fig. 8). Coastal and monsoon-dominated districts such as Cuddalore, Nagapattinam, Mayiladuthurai, Chengalpattu, Thanjavur and Thiruvallur exhibited comparatively higher POD and CSI values, indicating improved capability of SPPs in detecting heavy rainfall events associated with NEM and Bay of Bengal cyclonic disturbances, whereas inland semi-arid districts including Dharmapuri, Krishnagiri, Salem, Karur and Tirupathur showed relatively poor detection skill with low POD and CSI values. Among the evaluated products, MSWEP consistently demonstrated comparatively superior performance with higher POD and CSI values and relatively lower FAR values across several districts, suggesting improved robustness in capturing extreme rainfall occurrence. Similar findings were reported (21), who observed improved rainfall estimation capability of MSWEP over complex climatic regions. IMERG exhibited moderate agreement with observed rainfall patterns and generally outperformed CHIRPS, while CHIRPS showed comparatively higher FAR values, indicating increased false alarm occurrence and uncertainty during intense precipitation events.

© The Author(s) 2026. Creative Commons CC BY 4.0. Published by Horizon e-Publishing Group.
https://doi.org/10.14719/pst.16504



Fig. 7. Station-wise frequency of high rainfall events across Tamil Nadu based on Indian Meterological Department (IMD) classification (1998–2023).





© The Author(s) 2026. Creative Commons CC BY 4.0. Published by Horizon e-Publishing Group.
https://doi.org/10.14719/pst.16504

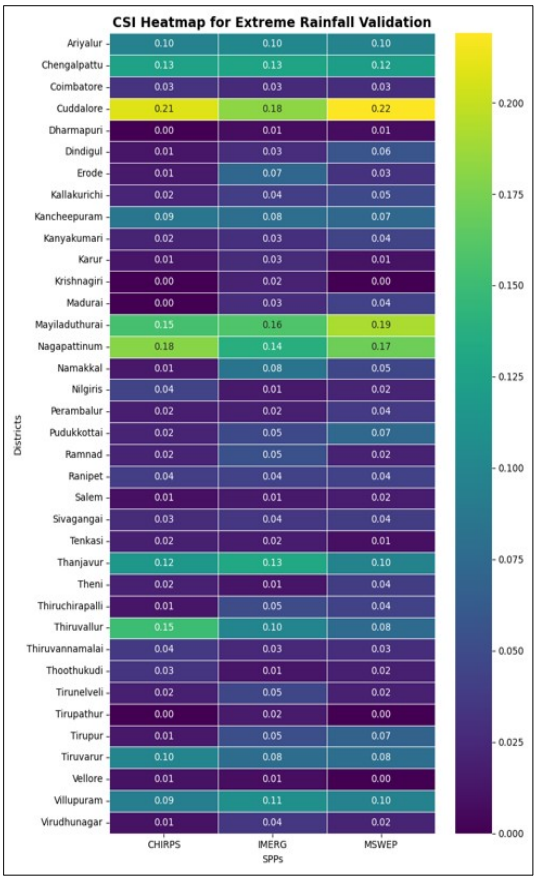


Fig. 8. Heatmap of extreme-event detection accuracy for Climate Hazards Center Infrared Precipitation with Stations (CHIRPS), Integrated Multi-satellite Retrievals for Global Precipitation Measurement (IMERG) and Multi-Source Weighted-Ensemble Precipitation (MSWEP).

The categorical verification metrics show that the three rainfall products for detection of the rainfall events over the study area is relatively limited (Fig. 9). The POD values varied from very low near 0.00–0.30. However, FAR values are consistently high (0.50–1.00), indicating that many detected rainfall events were not confirmed by ground observations. Similarly, the CSI values range from 0.00–0.22 indicating a generally low skill in the correct identification of rainfall events after accounting for both missed detections and false alarms. The median POD and CSI are slightly higher for IMERG and MSWEP than for CHIRPS, but the differences among the three datasets are relatively small. The larger interquartile ranges and several outliers indicate a considerable spatial variability in rainfall detection performance across the validation stations. The variability is likely associated with the complex rainfall characteristics of Tamil Nadu including localised convective storms, coastal influences and orographic effects of Western Ghats. Although the retrieval algorithms and spatial resolution differ, all the three products exhibit similar performance patterns, implying that the uncertainties are mainly associated with the intrinsic difficulty of retrieving localised rainfall events with high accuracy.

Performance assessment on seasonal precipitation estimates

Statistical evaluation

Evaluation of SPPs at the seasonal scale is crucial for assessing their performance across regions influenced by complex monsoon dynamics. In Tamil Nadu, the SWM and NEM seasons play an important role in influencing rainfall distribution patterns and their reliable prediction is fundamental for hydrological applications and climate impact assessments. CHIRPS, IMERG and MSWEP were analysed using both continuous and categorical performance metrics as represented in Table 10.

Table 10. Performance assessment of CHIRPS, IMERG and MSWEP at different seasons

1998–2023		RMSE (mm)	Correlation	PBIAS (%)	POD	FAR	CSI
	CHIRPS	197.7	0.43	47.5	0.582	0.745	0.213
SWM	IMERG	202.8	0.47	65.2	0.579	0.755	0.206
	MSWEP	156.8	0.53	35.0	0.729	0.725	0.249
NEM	CHIRPS	200.9	0.66	19.0	0.590	0.514	0.361

© The Author(s) 2026. Creative Commons CC BY 4.0. Published by Horizon e-Publishing Group.
https://doi.org/10.14719/pst.16504

IMERG	205.2	0.62	-13.1	0.562	0.554	0.332
MSWEP	183.4	0.69	2.6	0.817	0.522	0.430

POD: probability of detection; FAR: false alarm ratio; CSI: critical success index; CHIRPS: Climate Hazards Group Infrared Precipitation with Stations; IMERG: Integrated Multi-Satellite Retrievals for Global Precipitation Measurement; MSWEP: Multi-Source Weighted-Ensemble Precipitation.

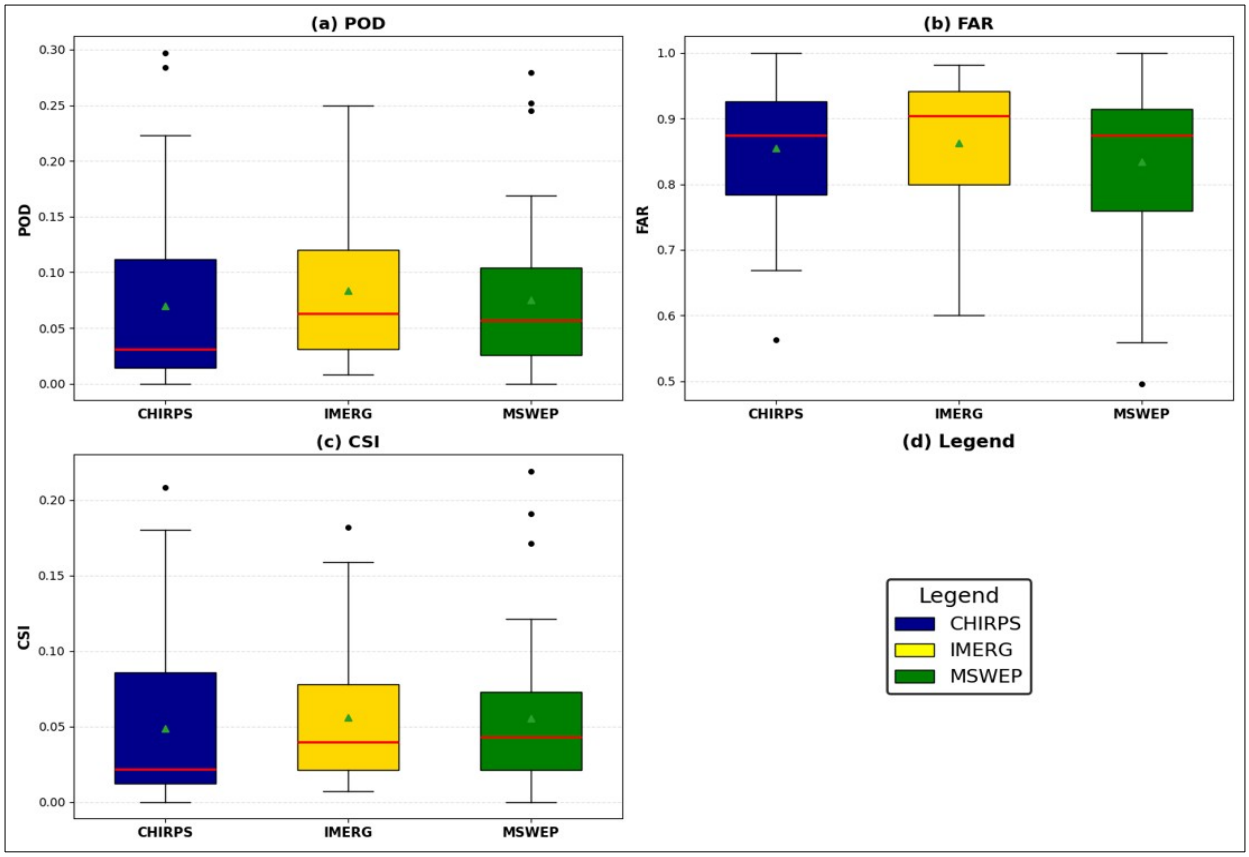


Fig. 9. Box plots of categorical detection metrics for extreme rainfall event verification across satellite-based precipitation products (SPPs) from 1998–2023.

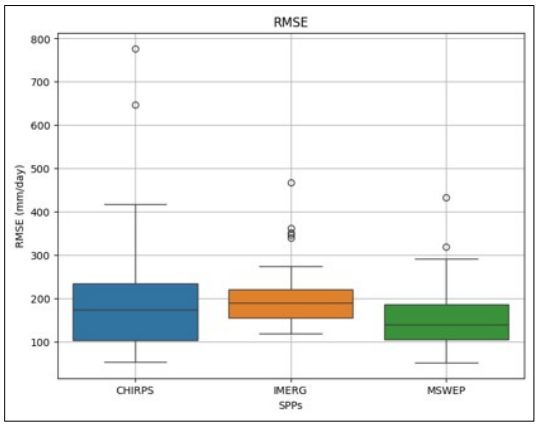
MSWEP indicated superior performance in terms of rainfall estimation and detection in Tamil Nadu during both SWM and NEM seasons. For SWM, MSWEP with RMSE of 156.8 mm, maximum correlation of 0.53 and minimum PBIAS of 35.0 % and the highest skill measures with POD of 0.729, minimum FAR of 0.725 and highest CSI of 0.249. This shows that the MSWEP performed better than the other two datasets, having less error and minimum positive bias than CHIRPS and IMERG that exhibited high errors and positive biases. A similar trend was witnessed during NEM, with MSWEP performing better through the minimum RMSE of 183.4 mm, maximum correlation of 0.69 and balanced PBIAS of 2.60 %, along with highest POD of 0.817, minimum FAR of 0.522 and maximum CSI of 0.430. In contrast, the CHIRPS underestimated rainfall amount and IMERG showed mixed bias and low detection skill. From this seasonal performance evaluation, it is clear that MSWEP is the best performing SPPs among all for both periods. As illustrated in Fig. 10, the dispersion and central tendency measures of the statistical indicators have been provided with 95 % confidence interval providing a measure of uncertainty, consistency and reliability of each product on a seasonal basis.

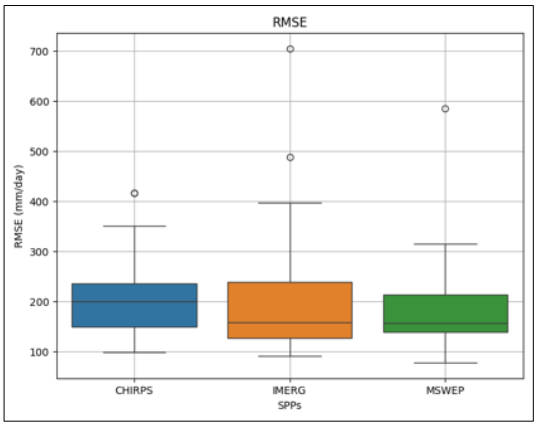
Pairwise Wilcoxon signed-rank tests showed that MSWEP's seasonal superiority was statistically significant for detection skill in both monsoon seasons as explained in Table 11, since POD, FAR (except for CHIRPS–MSWEP in NEM) and CSI were significantly different from zero for MSWEP compared to both of the other products ($p < 0.05$; Table 11). For PBIAS, all three pairwise comparisons were significantly different from zero in NEM ($p < 0.001$), thus highlighting the large differences in bias during cyclone-dominated rainfall, while only IMERG–MSWEP was significantly different in SWM ($p = 0.352$), although MSWEP had the lowest mean bias. Finally, for the continuous model evaluation measures, MSWEP's lead over CHIRPS in terms of RMSE and CC was statistically significant in SWM ($p = 0.011$ and $p < 0.001$), but not in NEM ($p = 0.071$ and $p = 0.353$), suggesting that MSWEP's benefits over CHIRPS are more prominent in the orographically-influenced SWM than in the synoptically-dominated NEM.

© The Author(s) 2026. Creative Commons CC BY 4.0. Published by Horizon e-Publishing Group.
https://doi.org/10.14719/pst.16504

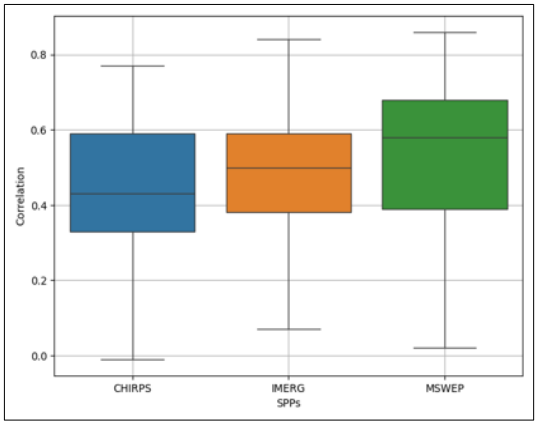
SWM NEM

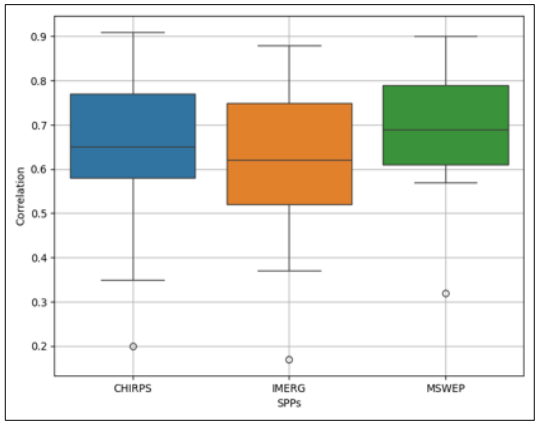
RMSE



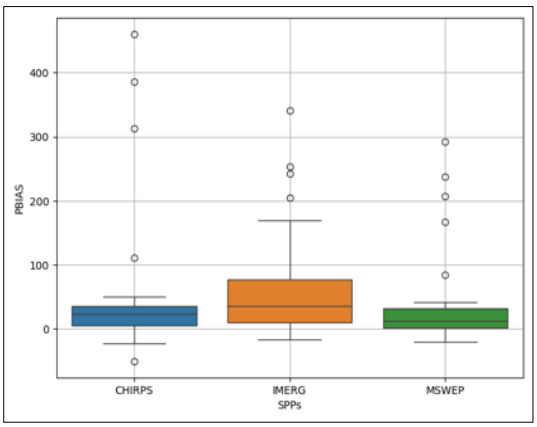


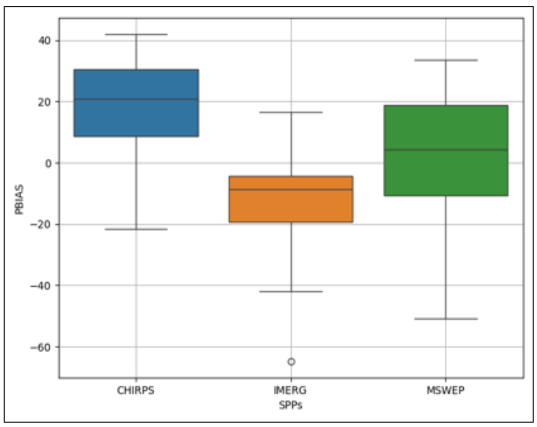
Correlation



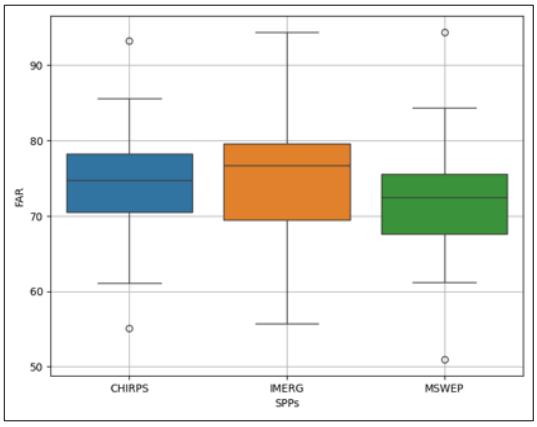


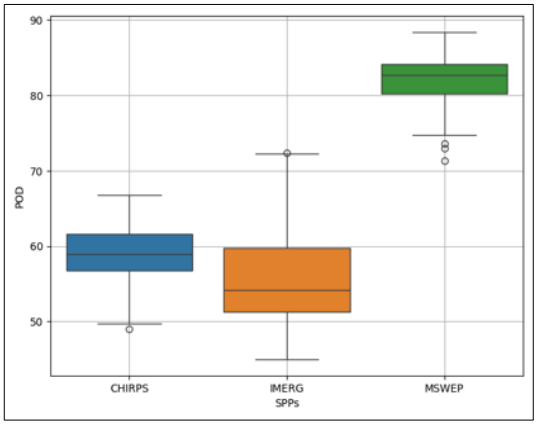
PBIAS





POD





© The Author(s) 2026. Creative Commons CC BY 4.0. Published by Horizon e-Publishing Group.
https://doi.org/10.14719/pst.16504

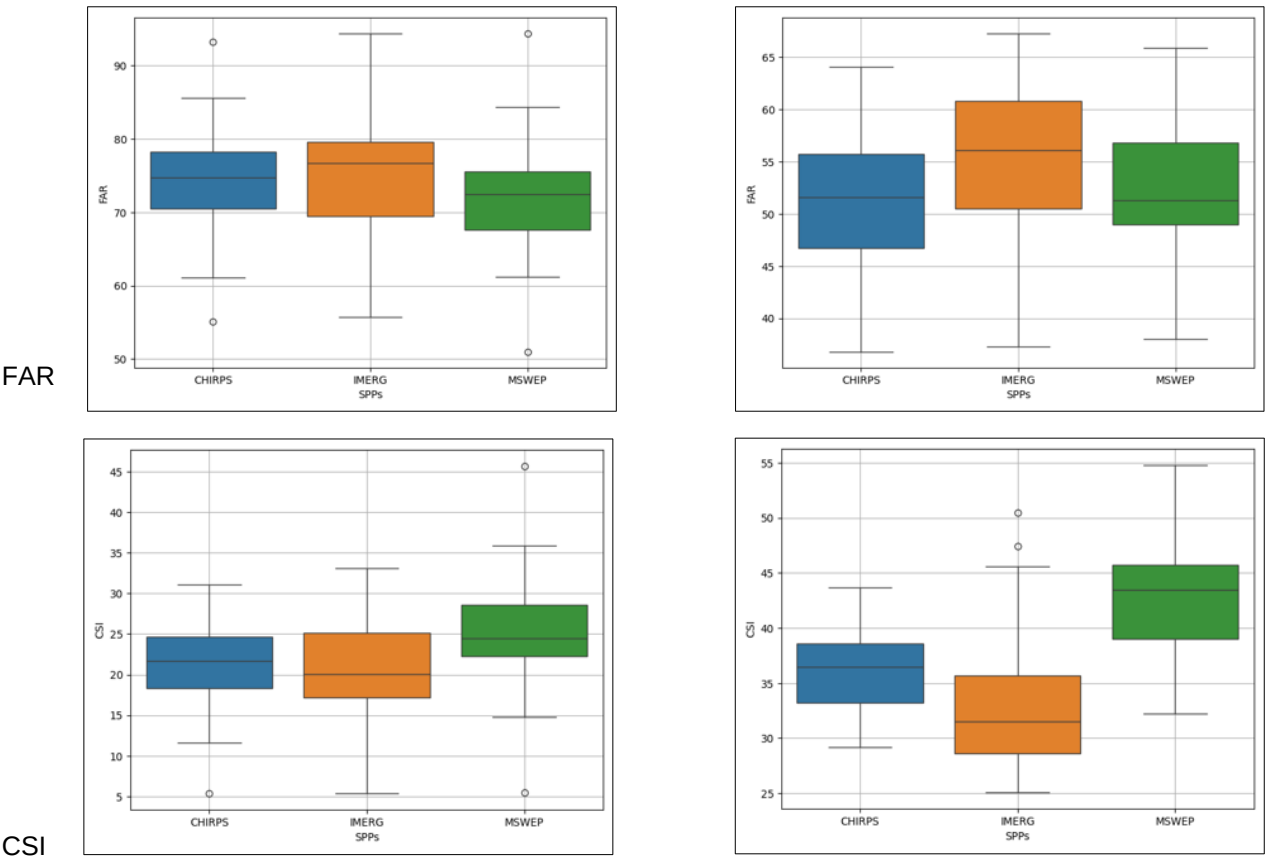


Fig. 10. Seasonal comparison of rainfall accuracy and detection skill across satellite-based precipitation products (SPPs) from 1998–2023.

Table 11. Pairwise Wilcoxon signed-rank test results at seasonal scale

Metric	Comparison	SWM		NEM	
		W	p (Bonf.)	W	p (Bonf.)
RMSE	CHIRPS vs IMERG	324.0	1.000 (ns)	300.0	0.627 (ns)
RMSE	CHIRPS vs MSWEP	162.0	0.011 (*)	228.0	0.071 (ns)
RMSE	IMERG vs MSWEP	95.0	0.0001 (**)	264.5	0.240 (ns)
CC	CHIRPS vs IMERG	254.5	0.430 (ns)	254.5	0.965 (ns)
CC	CHIRPS vs MSWEP	81.5	0.0001 (**)	219.5	0.353 (ns)
CC	IMERG vs MSWEP	225.5	0.274 (ns)	155.0	0.016 (*)
PBIAS	CHIRPS vs IMERG	261.0	0.530 (ns)	1.0	<0.001 (**)
PBIAS	CHIRPS vs MSWEP	247.0	0.352 (ns)	29.0	<0.001 (**)
PBIAS	IMERG vs MSWEP	72.0	<0.001 (**)	30.0	<0.001 (**)
POD	CHIRPS vs IMERG	311.0	1.000 (ns)	242.5	0.300 (ns)
POD	CHIRPS vs MSWEP	2.0	<0.001 (**)	0.0	<0.001 (**)
POD	IMERG vs MSWEP	7.0	<0.001 (**)	0.0	<0.001 (**)
FAR	CHIRPS vs IMERG	196.0	0.057 (ns)	28.0	<0.001 (**)
FAR	CHIRPS vs MSWEP	87.0	<0.001 (**)	251.0	0.388 (ns)
FAR	IMERG vs MSWEP	9.5	<0.001 (**)	71.5	0.0001 (**)
CSI	CHIRPS vs IMERG	206.0	0.223 (ns)	140.5	0.004 (**)
CSI	CHIRPS vs MSWEP	6.5	<0.001 (**)	3.5	<0.001 (**)
CSI	IMERG vs MSWEP	3.0	<0.001 (**)	0.0	<0.001 (**)

POD: probability of detection; FAR: false alarm ratio; CSI: critical success index; CHIRPS: Climate Hazards Group Infrared Precipitation with Stations; IMERG: Integrated Multi-Satellite Retrievals for Global Precipitation Measurement; MSWEP: Multi-Source Weighted-Ensemble Precipitation; NEM: Northeast monsoon; SWM: Southwest monsoon.

© The Author(s) 2026. Creative Commons CC BY 4.0. Published by Horizon e-Publishing Group.
https://doi.org/10.14719/pst.16504

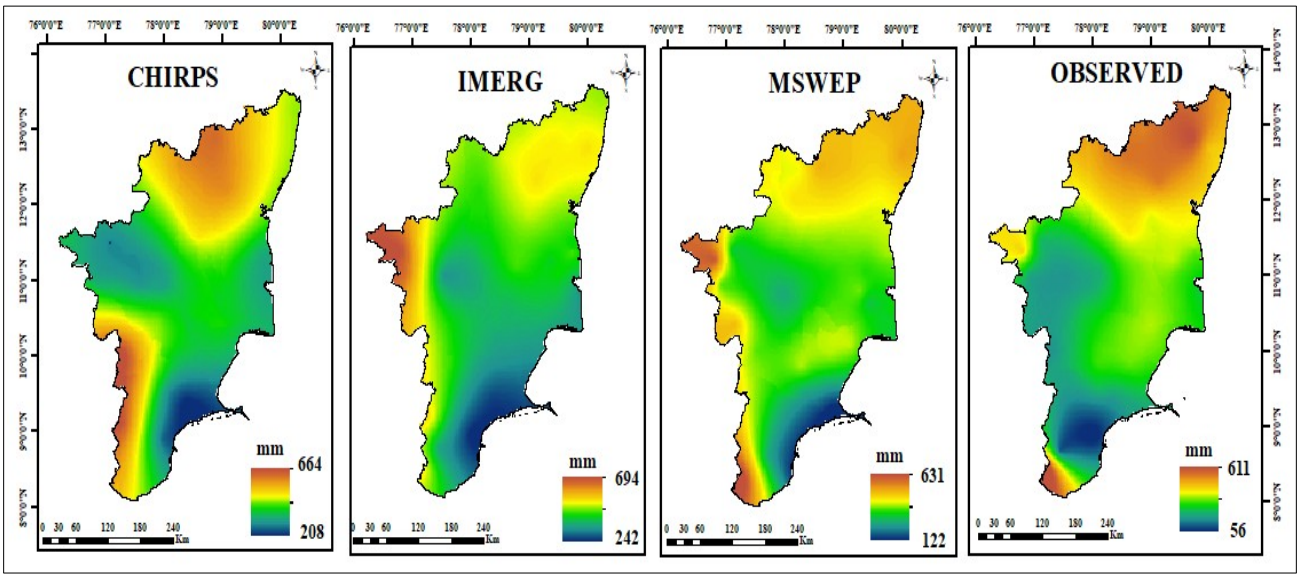
During SWM, the three SPPs showed different behaviours with respect to the statistically significant capturing of spatially heterogeneous precipitation in terms of RMSE with values between 52 mm and 777 mm with their median values of CHIRPS at 172.1 mm (CI: 149.1–246.3 mm), IMERG 189.1 mm (CI: 176.3–229.3 mm) and MSWEP lowest at 140 mm (CI: 130.9–182.6 mm). The correlation coefficient was between -0.01 and 0.84 for each SPP, in which MSWEP has highest median value of 0.58 (CI: 0.47–0.60), followed by IMERG of 0.50 (CI: 0.41–0.53) and CHIRPS of 0.43 (CI: 0.37–0.49) demonstrating high skill again because gauges and satellite often disagree on their estimates of the precipitation. Bias statistics confirmed that systematic overestimation in CHIRPS ranged from -50.3 to + 460.5 % (CI: 11.8–83.2%) and IMERG from -16.1–340.7 % (CI: 38.0–92.4 %), while MSWEP maintained lower bias (CI: 11.0–59.0 %) which ranged from -20–292.1 %. With regard to POD, MSWEP had the highest values of 0.61–0.91 (CI: 0.70–0.75), which was also seen for the value of fraction of false alarm from 0.51–0.94 (CI: 0.70–0.75) that indicates few false alarms similarly, CSI favoured MSWEP values between 0.05 and 0.46 (CI: 0.23–0.27), confirming its balanced skill in both accuracy and event detection followed by IMERG and CHIRPS.

During NEM (October–December), characterised by the presence of cyclonic events coupled with heavy rainfall along coastlines, there was a clear hierarchy of performance for the SPPs as the RMSE value range fell within 90.9–704.9 mm, with MSWEP always taking the lower ranks ranged from 77.6v585 mm (CI: 153.1–213.7). MSWEP recorded the highest correlation coefficient ranging from 0.32–0.90 (CI: 0.65–0.74) revealed stronger agreement; followed by CHIRPS (CI: 0.61–0.71) and IMERG (CI: 0.57–0.67). It was during the NEM period that the magnitude of bias became clearer, with CHIRPS showing significant positive bias (22–48 %), IMERG exhibiting inconsistent bias (underestimating or slightly overestimating) between −10 % and +15 %, while MSWEP performed better as it recorded the least biases (5–18 %). POD varied between 0.45 and 0.72 and the best detection was performed by MSWEP ranged from 0.71–0.88 (CI: 0.80–0.83). Similarly, the FAR measures (0.37–0.67) were lowest for MSWEP values between 0.38 and 0.66 (CI: 0.50–0.54), showing that there were less false detections of rainfall events. Also, the CSI (0.25–0.51) measure showed superiority in MSWEP ranged between 0.32–0.55 (CI: 0.41–0.45) demonstrating better detection capability followed by CHIRPS and IMERG.

Spatial distribution of seasonal rainfall

The spatial-temporal variations in seasonal rainfall play a crucial role in understanding the ability of various SPPs dataset to capture geographical variation in monsoonal rainfall over Tamil Nadu. The comparison between CHIRPS, IMERG and MSWEP with observed station measurements will reveal the spatial characteristics, bias within regions and advantages of each dataset in terms of capturing rainfall gradients as represented in Fig. 11.

During the SWM (June–September), CHIRPS and IMERG estimated higher rainfall totals (208–694 mm), while MSWEP produced slightly lower but more consistent values (122–631 mm) that closely matched station observations (56–611 mm). MSWEP's lower bias and stronger correlation highlight its resilience in orographic zones such as the Western Ghats, where satellite retrievals often struggle. CHIRPS and IMERG tended to overestimate rainfall in interior districts, reducing their reliability for hydrological applications. During NEM (October–December), which is Tamil Nadu's dominant rainfall season where coastal and deltaic districts will be receiving intense precipitation. CHIRPS recorded the highest totals (335–1100 mm), often overestimating coastal rainfall, while IMERG underestimated peak rainfall zones (250–783 mm). MSWEP provided balanced estimates (243–867 mm), closely aligning with station data (267–1010 mm), particularly in cyclone-prone regions such as Nagapattinam and Cuddalore.



SWM

© The Author(s) 2026. Creative Commons CC BY 4.0. Published by Horizon e-Publishing Group.
https://doi.org/10.14719/pst.16504

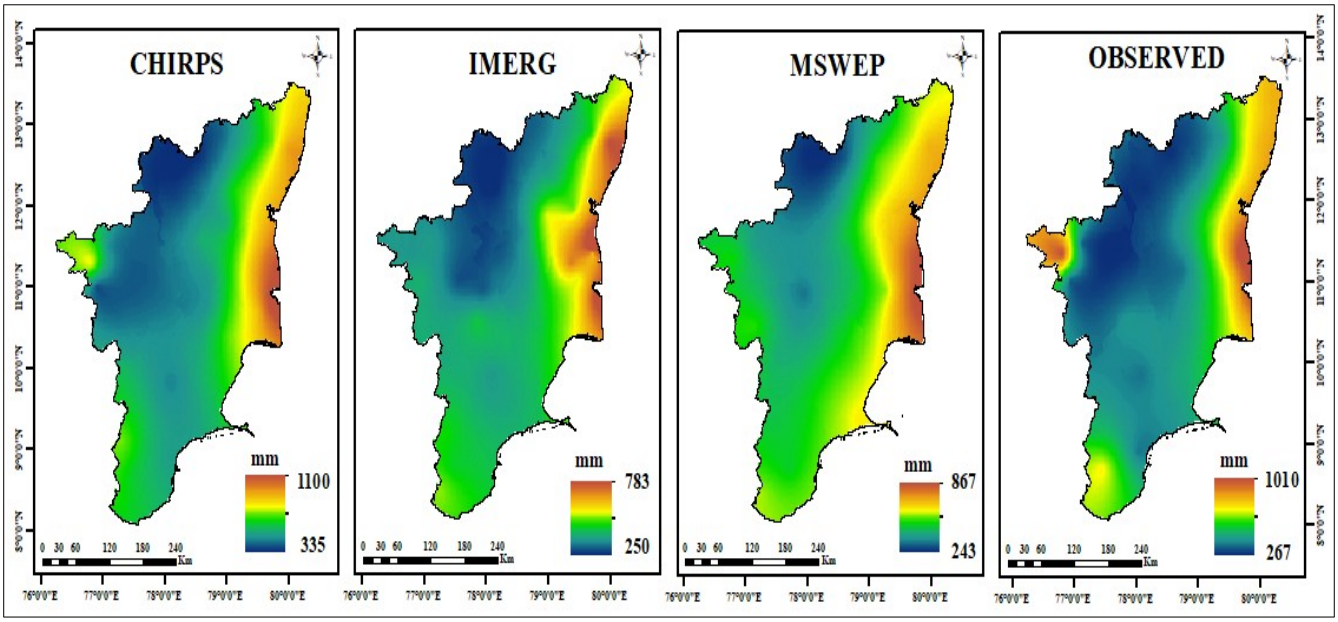


Fig. 11. Spatial distribution of mean seasonal rainfall of Tamil Nadu from 1998–2023 of different satellite products and observed stations.

Station-level seasonal rainfall variability

The station-based heatmap comparison of seasonal mean rainfall from 1998–2023 reveals distinct spatial and dataset-driven variability across Tamil Nadu during the SWM and NEM as represented in Fig. 12. SWM totals are generally higher in western and southern high-rain stations such as Nilgiris, Theni and Tirunelveli, where gridded products like CHIRPS and IMERG often show wet biases relative to observed station totals, particularly at high-rain sites; NEM totals peak at coastal and deltaic stations such as Nagapattinam, Cuddalore and Ramanathapuram, where products like MSWEP and CHIRPS sometimes align more closely with observed values. The largest spatial mismatches occur in cyclone-prone coastal belts (Nagapattinam, Cuddalore, Mayiladuthurai) and steep orographic gradients, where CHIRPS' coastal bias and IMERG's underestimation of extremes limit their utility for flood-sensitive applications. While MSWEP shows closer spatial coherence with observed patterns, consistent with regional validations reporting reduced bias in complex terrain.

Performance diagram analysis

The performance diagrams show seasonally distinct detection skill values as represented in Fig. 13. During the SWM, most points cluster in the moderate POD (≈ 0.55–0.75) and low to moderate success ratio (≈ 0.20 –0.45) region, indicating reasonable rainfall detection but with noticeable false alarms. MSWEP generally occupies higher POD and slightly better success ratios, translating to higher CSI values, while IMERG shows moderate performance and CHIRPS displays lower POD and wider scatter, reflecting larger station-to-station variability. In contrast, the NEM diagram shows a clear shift toward higher POD (≈ 0.60–0.85) and improved success ratios (≈ 0.40–0.65) for all products, indicating enhanced rainfall detection and fewer false alarms during the dominant rainfall season of Tamil Nadu. MSWEP consistently clusters in the region of highest POD and success ratio, corresponding to the highest CSI isolines, followed by IMERG, while CHIRPS remains comparatively lower but still shows improved skill relative to SWM.

Multi-timescale drought monitoring

The capability of SPI to describe both short-term droughts in meteorology and hydrological droughts were characterised using multi-temporal scale droughts analysis showing high variability in hydroclimatic conditions in Tamil Nadu from 1991–2023 (Fig. 14). Various stages of droughts were found to occur between 1991–93, 2002–04, 2012–16 and 2018–20 while relatively wet conditions prevailed between 1996–2001, 2006–12 and 2021–23, thus pointing out alternating dry and wet climatic periods during the whole study period based on drought severity classification. The period 2002–04 can be considered the longest drought period as indicated by SPI-24 and SPI-48 falling to around -1.20 to -1. The maximum positive anomalies occurred between 2021 and 2023 when the SPI-24 and SPI-48 values exceeded +1.45, which corresponds to moderately wet to severely wet categories and represents the recovery of rainfall during the latter part of the study period. Likewise, the negative SPI anomalies occurring in 2012, 2015–16 and 2018–20 represent the drought episodes caused by low monsoon rainfall amounts. The yearly variations of SPI-3 and SPI-6 were much higher because of their sensitivity to short-term rainfall anomalies, whereas SPI-24 and SPI-48 demonstrated smooth time behaviour, based on their integration of cumulative precipitation anomalies over long periods.

© The Author(s) 2026. Creative Commons CC BY 4.0. Published by Horizon e-Publishing Group.
https://doi.org/10.14719/pst.16504

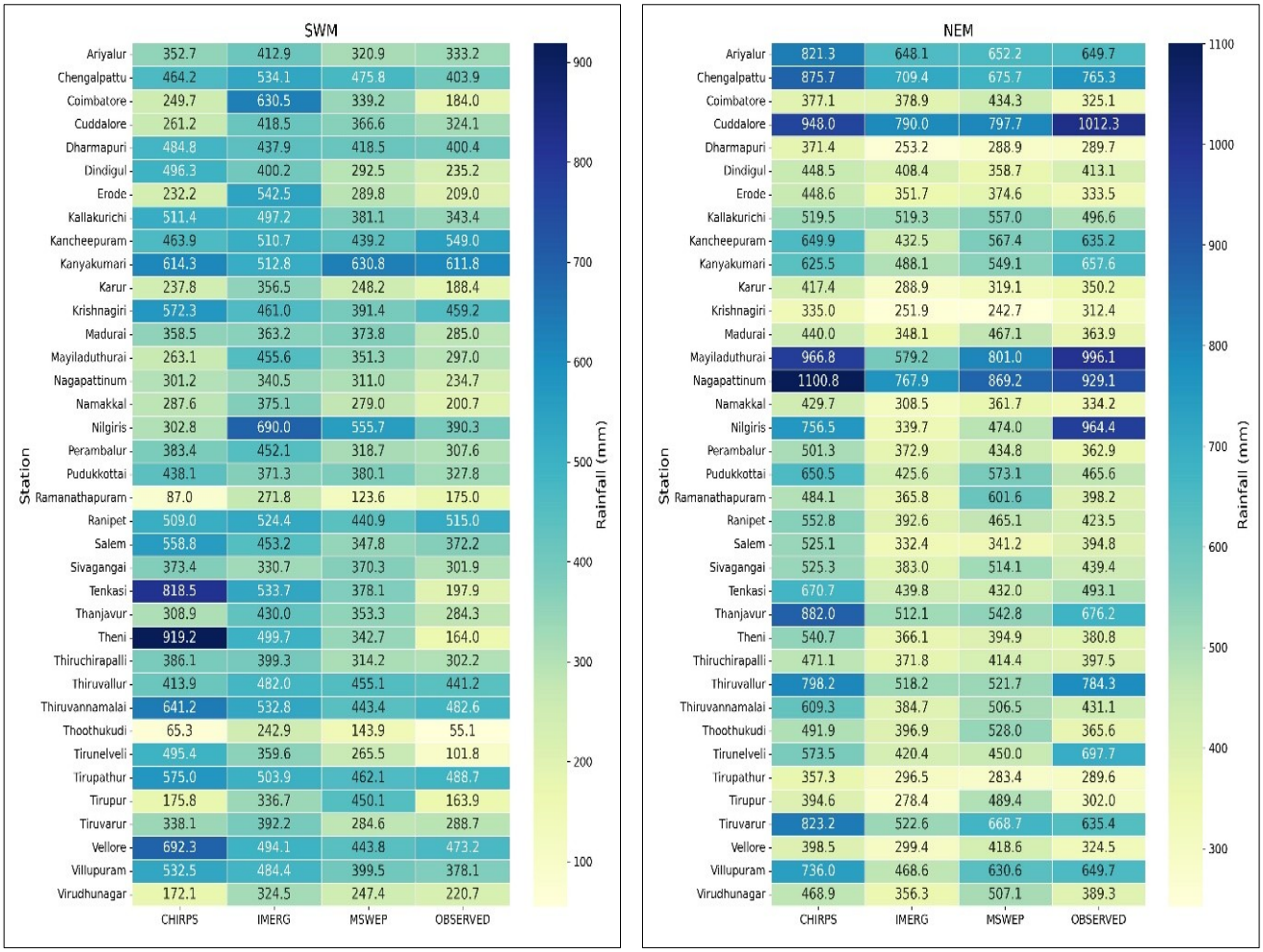


Fig. 12. Station-based heat map comparison of seasonal mean rainfall from 1998–2023 for Southwestern monsoon (SWM) and Northeast monsoon (NEM).

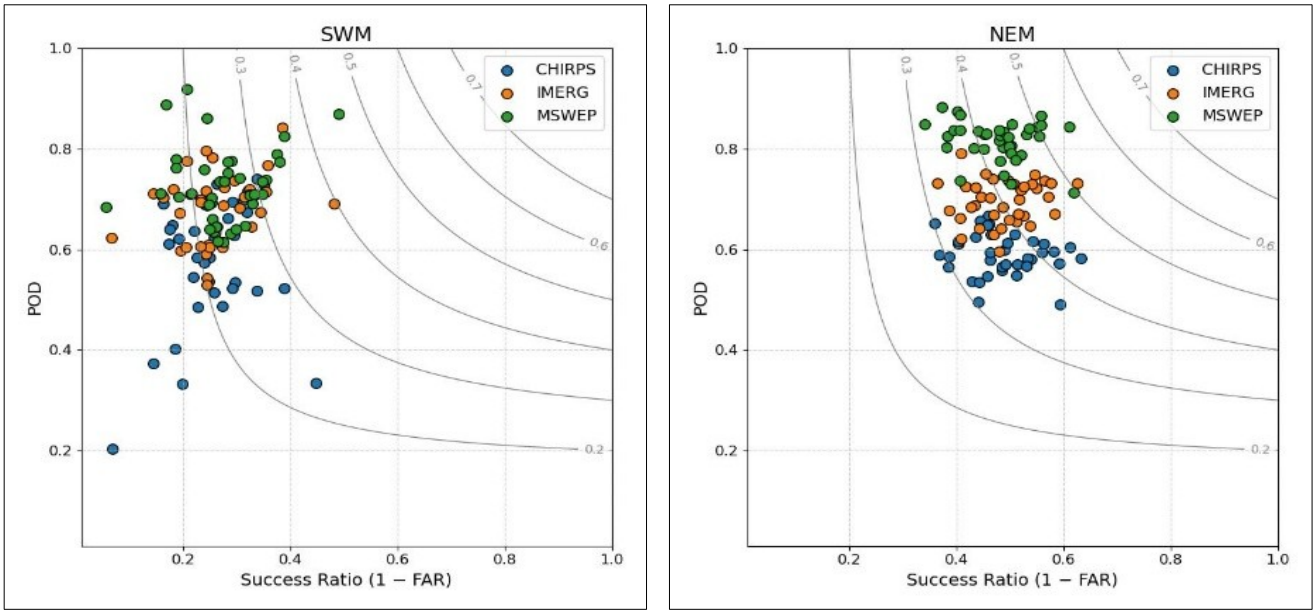


Fig. 13. Categorical performance diagram evaluating rainfall detection skill across Southwestern monsoon (SWM) and Northeast monsoon (NEM).

© The Author(s) 2026. Creative Commons CC BY 4.0. Published by Horizon e-Publishing Group.
https://doi.org/10.14719/pst.16504

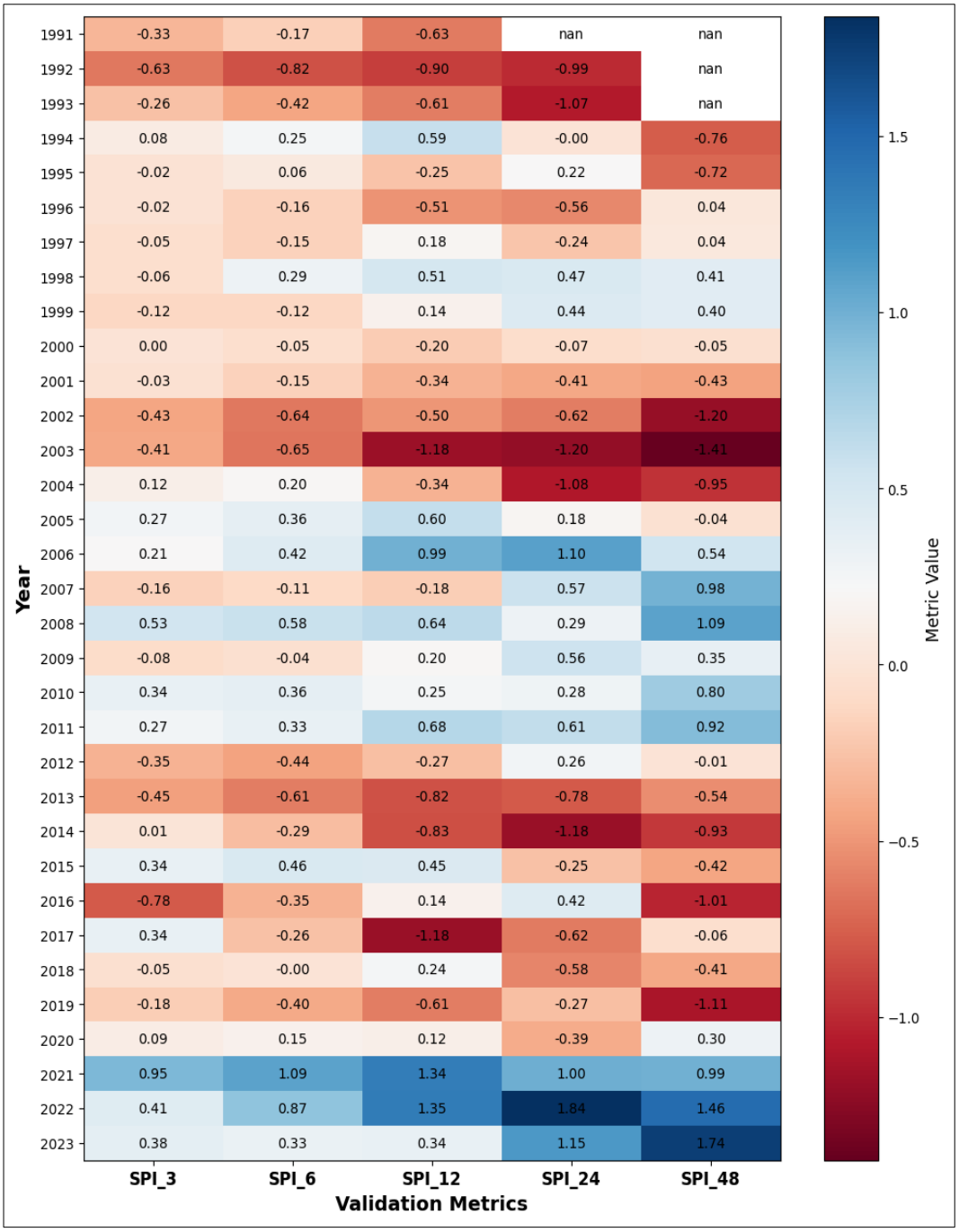


Fig. 14. Temporal heatmap of multi-timescale standardised precipitation index (SPI) values from 1991–2023.

These temporal features were further supported by the long-term frequency distribution of SPI categories, which showed that near normal hydroclimatic conditions predominated across the research period (Table 12). Near Normal circumstances accounted for 65.98–67.98 % of all observations over all accumulation periods, suggesting that precipitation was within the climatological normal range for the majority of years despite the occurrence of intermittent wet spells and droughts. Moderately wet circumstances made up the largest percentage of the wetness categories (8.72–10.81 %), followed by very wet (4.17–4.72 %) and extremely wet (1.75–2.75 %), indicating that moderate rainfall surpluses were significantly more often than extreme wet events. Similarly, the drought category that occurred most frequently was the moderate drought category, which occurred 8.85–10.05 % of the time. Moderate deficits in precipitation occurred much more frequently compared to severe and intense drought events, where moderate deficits occurred 50 % of the time, severe 4.17–5.58 % of the time and extreme drought 1.06–2.66 % of the time. Moreover, the percentage of occurrences of moderate drought and severe drought increased with increasing SPI accumulation periods, implying that prolonged periods of time tend to capture moisture deficits. From the findings, it can be concluded that there are moderate drought conditions in Tamil Nadu, which is usually associated with long recurrence, while extremely rare droughts can occur in this region.

© The Author(s) 2026. Creative Commons CC BY 4.0. Published by Horizon e-Publishing Group.
https://doi.org/10.14719/pst.16504

Table 12. Frequency distribution of standardised precipitation index (SPI)-based drought and wetness categories derived from the validated MSWEP precipitation dataset

Counts (Nos.)	Extremely wet	Very wet	Moderately wet	Near normal	Moderate drought	Severe drought	Extreme drought
SPI-3	2989	6957	14577	100177	13079	6146	3431
SPI-6	2566	6091	15803	98153	13134	6803	3684
SPI-12	2635	6287	13958	97331	12748	7198	3833
SPI-24	3582	6093	12160	93987	13678	7744	2258
SPI-48	308	473	1113	7403	1178	626	119
(%)	**Extremely wet**	**Very wet**	**Moderately wet**	**Near normal**	**Moderate drought**	**Severe drought**	**Extreme drought**
SPI-3	2.03	4.72	9.89	67.98	8.88	4.17	2.33
SPI-6	1.75	4.17	10.81	67.12	8.98	4.65	2.52
SPI-12	1.83	4.37	9.69	67.6	8.85	5	2.66
SPI-24	2.57	4.37	8.72	67.37	9.8	5.55	1.62
SPI-48	2.75	4.22	9.92	65.98	10.5	5.58	1.06

Spatial distribution of drought frequency provided further evidence of considerable regional diversity within Tamil Nadu agro-climatic zones in terms of persistence and spatial vulnerability to drought conditions (Fig. 15). During all periods of SPI accumulation, moderate drought occupied the largest area; however, severe and extreme drought was limited but more persistent in inland areas. During all following SPI accumulation periods, the North Western zone continued to be the major drought prone area; after that, the Western zone and parts of the Southern zone where moderate, severe and extreme drought frequently occurred. These drought-prone areas are primarily found in the semi-arid interior and rain-shadow regions affected by the Western Ghats. These areas are more susceptible to drought due to higher evapotranspiration, lower and more variable monsoonal rainfall and a greater reliance on seasonal precipitation. With only a few isolated localised hotspots, the Cauvery Delta zone, Northeastern zone and high rainfall zone, on the other hand, mostly stayed in the very low to low drought-frequency classes. This indicates relatively favourable moisture conditions brought about by NEM rainfall, river irrigation systems and orographic precipitation. The transformation from short-term meteorological drought to long-term hydrological drought is further illustrated by a gradual shift from localised dryness patches at SPI-3 and SPI-6 to more spatially continuous drought patterns at SPI-24 and SPI-48.

Discussion

Comparative performance of CHIRPS, IMERG and MSWEP

As shown by its lower RMSE (11.2 mm), higher correlation coefficient (0.30), lower PBIAS (10.0 %), higher POD (0.753), lower FAR (0.656) and higher CSI (0.308), MSWEP consistently outperformed the other satellite precipitation products throughout Tamil Nadu, according to a comparative evaluation of CHIRPS, IMERG and MSWEP. MSWEP's multi-source weighted ensemble structure, which incorporates satellite estimates, rain gauge observations and reanalysis data to lower systematic errors and enhance rainfall representation, is responsible for its exceptional performance. By utilising the complementing capabilities of several data sources, the ensemble weighting approach used in MSWEP greatly enhances precipitation estimation (10, 38, 39). In contrast, IMERG had intermediate performance but more variability among physiographic regions, whereas CHIRPS demonstrated the biggest positive bias and lowest detection capabilities. Similar findings were previously reported, who observed that infrared-based products like CHIRPS typically show increased uncertainty under convective rainfall circumstances (11) and who discovered that IMERG performance declines in areas with complex terrain (9). Thus, in climatically complex environments like Tamil Nadu, ensemble-based precipitation products offer more accurate rainfall predictions than single-sensor datasets, according to the current findings.

Influence of monsoon systems

Precipitation estimation accuracy in Tamil Nadu is strongly influenced by physiography and monsoon dynamics, as seen by the spatial heterogeneity in satellite rainfall performance. The Western Ghats and coastal districts, where complicated terrain, orographic uplift and cyclonic rainfall systems produce extremely varied precipitation patterns, had higher RMSE values and lower correlations. Because rainfall intensity and distribution can fluctuate over short spatial scales, these conditions pose significant problems to satellite retrieval methods. Similar results were previously reported, who noted higher retrieval uncertainty in topographically complicated and hilly areas (13). Estimation errors are further influenced by Tamil Nadu's dual monsoon system, where the NEM produces widespread rainfall linked to cyclonic disturbances from the Bay of Bengal and the SWM produces localised orographic rainfall along the Western Ghats. MSWEP maintained more consistency throughout both monsoon seasons, despite the fact that all products performed better during NEM due to the greater spatial extent of rainfall systems (40, 41). This suggests that the inclusion of gauge observations and reanalysis data helps offset retrieval limitations in areas impacted by complex terrain and extreme weather conditions.

© The Author(s) 2026. Creative Commons CC BY 4.0. Published by Horizon e-Publishing Group.
https://doi.org/10.14719/pst.16504

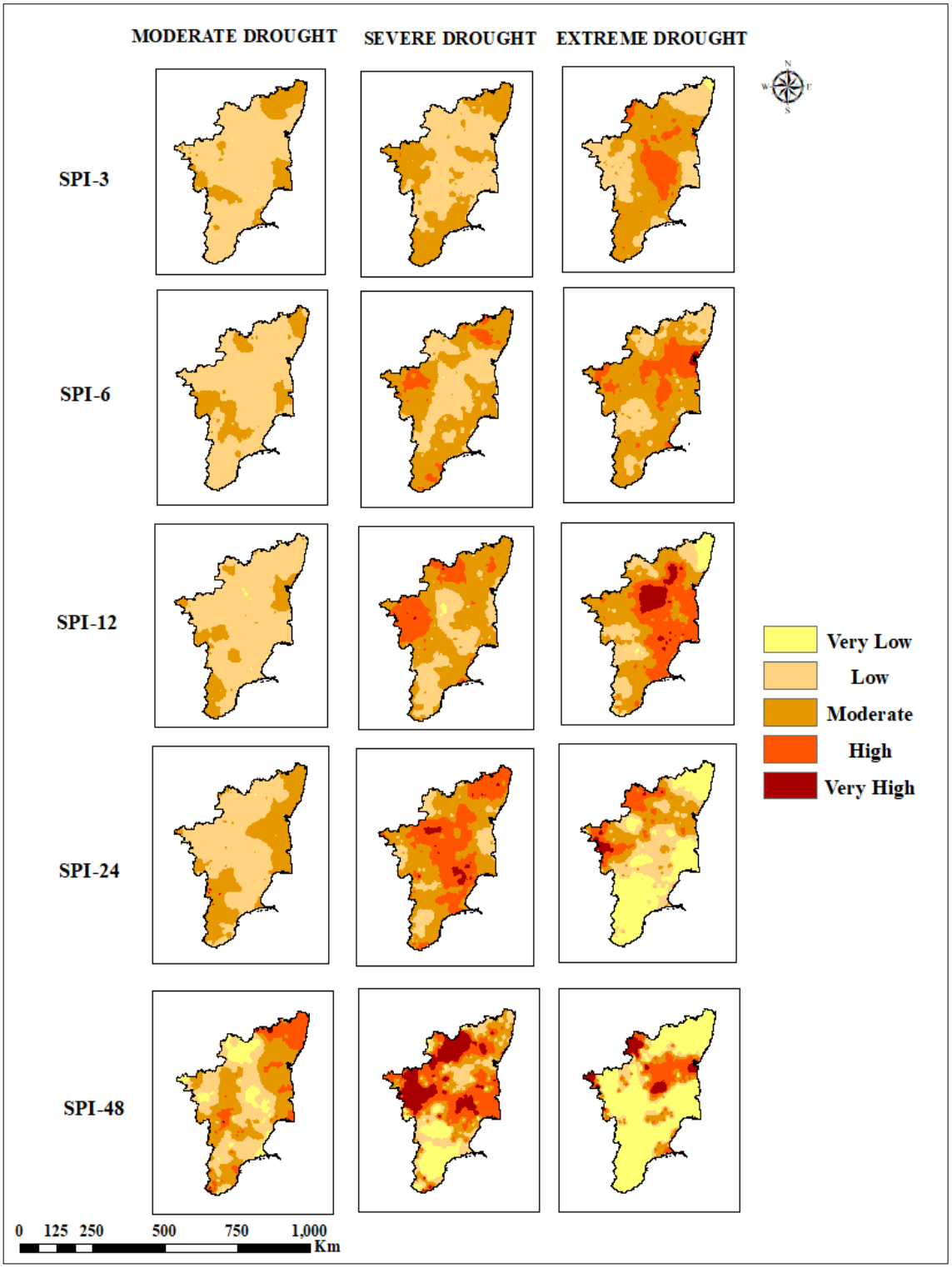


Fig. 15. Spatial distribution of drought occurrence frequency (%) derived from Multi-Source Weighted-Ensemble Precipitation (MSWEP).

Seasonal differences in satellite rainfall performance

Seasonal analysis of the capability of satellite-based rainfall products in reproducing the rainfall characteristics during the SWM season and the NEM season yielded varying results. Since convective and orographic rainfall are the dominant phenomena during SWM, higher errors and lower skill detection were recorded for all satellite precipitation products, especially those locations that had heavy rainfall such as Nilgiris, Theni and Tirunelveli. Higher wet biases and variability were noted with CHIRPS and IMERG, signifying difficulties in accurately recording precipitation because of terrain-related meteorological events. Previous results confirmed similar findings and emphasised the limits of satellite rainfall products in hilly regions (42). For NEM, there was a substantial improvement in the skill for detecting precipitation since precipitation is mostly a function of large synoptic systems and tropical

© The Author(s) 2026. Creative Commons CC BY 4.0. Published by Horizon e-Publishing Group.
https://doi.org/10.14719/pst.16504

cyclones, which are easily detectable from space-based platforms. However, MSWEP had the best performance in terms of the highest POD, lowest bias and maximum CSI. This indicates that MSWEP performs better in detecting rainfall variation throughout the year. This is supported by the early results showing that blended precipitation datasets have higher consistency and reliability owing to multiple information sources about precipitation (38, 39, 43).

Implications of multi-timescale drought monitoring for hydrological and agricultural application

Since the drought analysis is based on the validated MSWEP precipitation dataset, the residual uncertainty in the MSWEP estimates needs to be accounted for when interpreting the SPI-based drought classification. While it had the lowest RMSE (11.2 mm) and PBIAS (10 %), MSWEP had a consistent positive bias that increased during the SWM (up to 35 %) and was especially prominent over the Western Ghats and other mountainous areas. Due to the gamma distribution used to standardise the SPI, such a bias might be amplified depending on the duration of the drought. Therefore, the classifications near the critical −1.0 threshold (near normal or moderate drought) should be treated with caution over areas with large uncertainties. At the same time, since MSWEP had the lowest bias and the highest detection skill among the SPPs, droughts identified based on the SPI may still have sufficient reliability for the study area. In particular, the drought onset detected in Tamil Nadu using this dataset is likely to be considered at inter-annual timescales that are typically relevant for agricultural planning.

The application of multi-timescale SPI methodology along with MSWEP precipitation data provides a comprehensive approach for understanding drought dynamics and achieving climate resilient water resource management in Tamil Nadu. Adequate precipitation data are vital for an accurate determination of the onset, duration and termination of drought and the accuracy of MSWEP precipitation data has been shown during precipitation validation and further in SPI calculation. While the long-term indices (SPI-24 and SPI-48) reflect the cumulative precipitation shortages associated with groundwater levels, reservoir storage and hydrological stress within basins, the short-term indices (SPI-3 and SPI-6) can better detect seasonal variations in rainfall amounts and hence are suitable for the evaluation of meteorological and agricultural droughts. The same was observedwhich states that integrating multi-timescale SPI using accurate precipitation data greatly improves the ability to define droughts in various agro-climatic zones of Tamil Nadu (44). The semiarid interior region is more prone to droughts compared to the Cauvery Delta and high rainfall zones due to favourable monsoon rains, availability of irrigation facilities and geographical conditions that make droughts rare in these regions. The critical hydroclimatic problem faced by the state is that of cumulative seasonal moisture deficits, which is indicated by the predominance of recurrent mild drought conditions rather than extreme drought events. This brings out the importance of developing region-specific drought-mitigation measures. Meanwhile the importance of drought assessments across multiple timescales for sustainable water resource management in monsoon-influenced areas that greatly enhance drought monitoring, hydrological modelling, reservoir management and irrigation planning (45).

Limitations and future research

Although the present study provides an extensive evaluation of SPPs and drought characteristics across multiple timescales in the state of Tamil Nadu, it does have certain limitations that must be acknowledged. The data validation was done with the help of 37 long-term synoptic rain gauge stations, which might not be able to capture the small-scale variations in rainfall in physio graphically complex areas such as the Western Ghats, coastal and rain shadow zones, although they do cover the major agro climatic zones. It also does not evaluate the capacity of satellite products to capture sub-daily rainfall patterns associated with convective storms, cyclones and other high intensity events. Standardized precipitation index which only considers precipitation anomalies into consideration and neglects temperature, evapotranspiration, soil moisture and groundwater storage, which strongly influence drought dynamics under changing climate conditions. Despite the MSWEP performing better than other datasets analysed, there might be still uncertainties associated with precipitation measurements by satellites and interpolation that could play a role in assessing the drought at smaller scales where local impacts are very important.

Future research should integrate high-resolution datasets, advanced models and considering several drought indices that will increase accuracy of precipitation assessment and drought characterisation. Using weather radars data, GPM dual-frequency precipitation radar and downscaled reanalysis datasets for assessing satellite precipitation products on the sub-daily, weekly and monthly scales and thus results in a better understanding of rainfall variability and extreme precipitation events. In order to accurately estimate the progression of meteorological, agricultural and hydrological droughts in the future, SPI needs to be complemented by other drought indices, such as standardised precipitation evapotranspiration index (SPEI), standardised soil moisture index (SSI), normalized difference vegetation index (NDVI), vegetation condition index (VCI) and groundwater measurements. Furthermore, the application of machine learning algorithms such as Random Forest, XGBoost and Deep Learning in addition to climatic, topographic, hydrological and remote sensing parameters offers immense possibilities in terms of correcting biases in satellite rainfall estimates and prediction of droughts. Using predictions made by regional climate models (CMIP6) and drought early warning systems specific to agro-climatic zones, this approach will greatly help in climate adaptation, sustainable water resource management and drought-resilient agriculture in Tamil Nadu.

© The Author(s) 2026. Creative Commons CC BY 4.0. Published by Horizon e-Publishing Group.
https://doi.org/10.14719/pst.16504

Conclusion

Using long-term rain gauge measurements and multi-timescale drought analysis in Tamil Nadu, this study provides a comprehensive analysis of three widely used satellite rainfall products (Climate Hazards Center Infrared Precipitation with Stations (CHIRPS), Integrated Multi-satellite Retrievals for Global Precipitation Measurement (IMERG) and Multi-Source Weighted-Ensemble Precipitation (MSWEP)). As a result, an integrated system for rainfall validation and hydro-climate analysis was provided. With the lowest error, minimal systematic bias and high rainfall detection capability, MSWEP consistently outperformed other evaluated datasets in terms of simulated rainfall intensity and frequency. The regions that are the most vulnerable to drought in the state are the Northwestern, Western and Southern Agro-Climatic zones. The validated MSWEP dataset was utilised in multi-scale standardised precipitation index (SPI) analysis, which efficiently illustrated the process of droughts development from short-term meteorological to long-term hydrological drought. Recurring moderate drought conditions are more common, which suggests that cumulative seasonal moisture deficiencies represent a more significant long-term problem than isolated extreme drought instances. These results show that the reliability of hydrological modelling, drought early-warning systems, irrigation planning, reservoir operation and climate-risk assessment is significantly improved when validated multi-source precipitation products are integrated with multi-timescale drought indices. This study provides a framework for evaluating precipitation and monitoring drought in monsoon-dominated areas that remains both operationally and scientifically valid. This framework is useful for managing water resources efficiently and sustainably, planning agricultural practices that are resilient to climate change and developing evidence-based policies in the face of rising climatic variability.

Acknowledgements

The authors share and acknowledge their gratitude towards Chief Minister Research Fellowship (CMRF 2023) by the Directorate of Collegiate education provided by Higher education department of Tamil Nadu supported to develop the research on further successful steps. The authors acknowledge that the Tamil Nadu Agricultural University, Coimbatore in providing the technical support for the enhancement of this manuscript.

Authors' contributions

KKJD designed the experiments, conducted the study, performed data collection, literature review, data analysis and interpretation, prepared the original draft and revised the manuscript. PS contributed to manuscript review and editing and supervised the research. SNK contributed to conceptualisation, resource acquisition, manuscript review and editing and supervision. PPC contributed to conceptualisation, manuscript review and editing and overall supervision of the study. SAP contributed to manuscript review and editing. VG contributed to manuscript review and editing. All authors have read and approved the final manuscript.

Compliance with ethical standards

Conflict of interest

Authors do not have any conflict of interests to declare.

Ethical issues

None

Declaration of generative AI and AI-assisted technologies in the writing

During the preparation of this work the authors used GRAMMARLY in order to eliminate the grammatical writing errors. After using this tool/service, the author(s) reviewed and edited the content as needed and takes full responsibility for the content of the publication.

References

1. Landrum L, Holland MM. Extremes become routine in an emerging new Arctic. Nat Clim Chang. 2020;10(12):1108–15. https://doi.org/10.1038/s41558-020-0892-z
2. Wang Y, Shen J, Wang Y, Liu X, Cao X, Herzschuh U. Abrupt mid-Holocene decline in the Indian Summer Monsoon caused by tropical Indian Ocean cooling. Clim Dyn. 2020;55(7):1961–77. https://doi.org/10.1007/s00382-020-05363-7
3. Rathore LS, Pattanaik DR, Bhan SC. Weather extremes: a spatio-temporal perspective. Mausam. 2016;67(1):27–52. https://doi.org/10.54302/mausam.v67i1.1141
4. Khosravi H, Azareh A, Dameneh HE, Sardoii ER, Dameneh HE. Assessing the effects of climate change on land cover changes in different time periods. Arab J Geosci. 2017;10(4):93. https://doi.org/10.1007/s12517-017-2837-z
5. Dinku T, Funk C, Peterson P, Maidment R, Tadesse T, Gadain H, et al. Validation of the CHIRPS satellite rainfall estimates over eastern Africa. Q J R Meteorol Soc. 2018;144:292–312. https://doi.org/10.1002/qj.3244
6. Mohan Kumar S, Geethalakshmi V, Ramanathan S, Senthil A, Senthilraja K, Bhuvaneswari K, et al. Rainfall spatial-temporal variability and trends in the Thamirabharani River Basin, India: implications for agricultural planning and water management. Sustainability. 2022;14(22):14948. https://doi.org/10.3390/su142214948
7. Yin Z, Ottlé C, Ciais P, Zhou F, Wang X, Jan P, et al. Irrigation, damming and streamflow fluctuations of the Yellow River. Hydrol Earth Syst Sci. 2021;25(3):1133–50. https://doi.org/10.5194/hess-25-1133-2021
8. Funk C, Peterson P, Landsfeld M, Pedreros D, Verdin J, Shukla S, et al. The climate hazards infrared precipitation with stations—a new environmental record for monitoring

© The Author(s) 2026. Creative Commons CC BY 4.0. Published by Horizon e-Publishing Group.
https://doi.org/10.14719/pst.16504

extremes. Sci Data. 2015;2(1):150066. https://doi.org/10.1038/sdata.2015.66

9. Huffman GJ, Bolvin DT, Braithwaite D, Hsu K, Joyce R, Xie P, et al. NASA global precipitation measurement (GPM) integrated multi-satellite retrievals for GPM (IMERG): algorithm theoretical basis document (ATBD), version 4.4. 2015.

10. Beck HE, Van Dijk AI, Levizzani V, Schellekens J, Miralles DG, Martens B, et al. MSWEP: 3-hourly 0.25° global gridded precipitation (1979–2015) by merging gauge, satellite and reanalysis data. Hydrol Earth Syst Sci. 2017;21(1):589–615. https://doi.org/10.5194/hess-21-589-2017

11. Funk C, Verdin A, Michaelsen J, Peterson P, Pedreros D, Husak G. A global satellite-assisted precipitation climatology. Earth Syst Sci Data. 2015;7(2):275–87. https://doi.org/10.5194/essd-7-275-2015

12. Hou AY, Kakar RK, Neeck S, Azarbarzin AA, Kummerow CD, Kojima M, et al. The global precipitation measurement mission. Bull Am Meteorol Soc. 2014;95(5):701–22. https://doi.org/10.1175/BAMS-D-13-00164.1

13. Fang X, Guo X, Zhang C, Shao H, Zhu S, Li Z, et al. Contributions of climate change to the terrestrial carbon stock of the arid region of China: a multi-dataset analysis. Sci Total Environ. 2019;668:631–44. https://doi.org/10.1016/j.scitotenv.2019.02.408

14. Sharma S, Hamal K, Khadka N, Joshi BB. Dominant pattern of year-to-year variability of summer precipitation in Nepal during 1987–2015. Theor Appl Climatol. 2020;142(3):1071–84. https://doi.org/10.1007/s00704-020-03359-1

15. Sunilkumar K, Narayana Rao T, Saikranthi K, Purnachandra Rao M. Comprehensive evaluation of multisatellite precipitation estimates over India using gridded rainfall data. J Geophys Res Atmos. 2015;120(17):8987–9005. https://doi.org/10.1002/2015JD023437

16. Belay AS, Fenta AA, Yenehun A, Nigate F, Tilahun SA, Moges MM, et al. Evaluation and application of multi-source satellite rainfall product CHIRPS to assess spatio-temporal rainfall variability on data-sparse western margins of Ethiopian highlands. Remote Sens. 2019;11(22):2688. https://doi.org/10.3390/rs11222688

17. Gebremichael M, Bitew MM, Hirpa FA, Tesfay GN. Accuracy of satellite rainfall estimates in the Blue Nile Basin: lowland plain versus highland mountain. Water Resour Res. 2014;50(11):8775–90. https://doi.org/10.1002/2013WR014500

18. Ayele GT, Teshale EZ, Yu B, Rutherfurd ID, Jeong J. Streamflow and sediment yield prediction for watershed prioritization in the Upper Blue Nile River Basin, Ethiopia. Water. 2017;9(10):782. https://doi.org/10.3390/w9100782

19. Huffman GJ, Bolvin DT, Braithwaite D, Hsu KL, Joyce RJ, Kidd C, et al. Integrated multi-satellite retrievals for the Global Precipitation Measurement (GPM) mission (IMERG). In: Satellite precipitation measurement: Volume 1. Cham: Springer International Publishing; 2020. p. 343–53. https://doi.org/10.1007/978-3-030-24568-9_19

20. Tan J, Oreopoulos L. Subgrid precipitation properties of mesoscale atmospheric systems represented by MODIS cloud regimes. J Clim. 2019;32(6):1797–812. https://doi.org/10.1175/JCLI-D-18-0570.1

21. Beck HE, Wood EF, Pan M, Fisher CK, Miralles DG, Van Dijk AI, et al. MSWEP V2 global 3-hourly 0.1° precipitation: methodology and quantitative assessment. Bull Am Meteorol Soc. 2019;100(3):473–500. https://doi.org/10.1175/BAMS-D-17-0138.1

22. Saeedi M, Kim H, Nabaei S, Brocca L, Lakshmi V, Mosaffa H. A comprehensive assessment of SM2RAIN-NWF using ASCAT and a combination of ASCAT and SMAP soil moisture products for rainfall estimation. Sci Total Environ. 2022;838:156416.

23. Legates DR, McCabe GJ Jr. Evaluating the use of "goodness-of-fit" measures in hydrologic and hydroclimatic model validation. Water Resour Res. 1999;35(1):233–41. https://doi.org/10.1029/1998WR900018

24. Xu R, Tian F, Yang L, Hu H, Lu H, Hou A. Ground validation of GPM IMERG and TRMM 3B42V7 rainfall products over southern Tibetan Plateau based on a high-density rain gauge network. J Geophys Res Atmos. 2017;122(2):910–24. https://doi.org/10.1002/2016JD025418

25. Ratner B. The correlation coefficient: its values range between +1/-1, or do they? J Target Meas Anal Mark. 2009;17(2):139–42. https://doi.org/10.1057/jt.2009.5

26. Gupta AK, Nagar DK. Matrix variate distributions. Boca Raton (FL): Chapman and Hall/CRC; 2018. 348p. https://doi.org/10.1201/9780203749289

27. Zhou Z, Guo B, Xing W, Zhou J, Xu F, Xu Y. Comprehensive evaluation of latest GPM era IMERG and GSMaP precipitation products over mainland China. Atmos Res. 2020;246:105132. https://doi.org/10.1016/j.atmosres.2020.105132

28. Shen H, Wang Y, Jiang K, Li S, Huang D, Wu J, et al. Simulation modeling for effective management of irrigation water for winter wheat. Agric Water Manag. 2022;269:107720. https://doi.org/10.1016/j.agwat.2022.107720

29. Rozante JR, Vila DA, Barboza Chiquetto J, Fernandes AD, Souza Alvim D. Evaluation of TRMM/GPM blended daily products over Brazil. Remote Sens. 2018;10(6):882. https://doi.org/10.3390/rs10060882

30. Ebert EE. Methods for verifying satellite precipitation estimates. In: Measuring precipitation from space: EURAINSAT and the future. Dordrecht: Springer Netherlands; 2007. p. 345–56. https://doi.org/10.1007/978-1-4020-5835-6_27

31. Dinku T, Ruiz F, Connor SJ, Ceccato P. Validation and intercomparison of satellite rainfall estimates over Colombia. J Appl Meteorol Climatol. 2010;49(5):1004–14. https://doi.org/10.1175/2009JAMC2260.1

32. Wilks DS. Statistical methods in the atmospheric sciences. 3rd ed. Amsterdam: Academic Press; 2011. 704p. https://doi.org/10.1016/B978-0-12-385022-5.00001-4

33. Amjad M, Yilmaz MT, Yucel I, Yilmaz KK. Performance evaluation of satellite- and model-based precipitation products over varying climate and complex topography. J Hydrol. 2020;584:124707. https://doi.org/10.1016/j.jhydrol.2020.124707

34. Wilcoxon F. Individual comparisons by ranking methods. Biometrics Bull. 1945;1(6):80–3. https://doi.org/10.2307/3001968

35. Dunn OJ. Multiple comparisons among means. J Am Stat Assoc. 1961;56(293):52–64. https://doi.org/10.1080/01621459.1961.10482090

36. McKee TB, Doesken NJ, Kleist J. The relationship of drought frequency and duration to time scales. In: Proceedings of the 8th Conference on Applied Climatology. Boston (MA): American Meteorological Society; 1993. p. 179–83.

© The Author(s) 2026. Creative Commons CC BY 4.0. Published by Horizon e-Publishing Group.

https://doi.org/10.14719/pst.16504

37. Keyantash J. The climate data guide: standardized precipitation index (SPI). Boulder (CO): National Center for Atmospheric Research; 2018.

38. Singh M, Rath BS. Rainfall characteristics under changing climate in Sundergarh district of Odisha. Mausam. 2024;75(4):993–1008. https://doi.org/10.54302/mausam.v75i4.3563

39. Beck HE, Pan M, Roy T, Weedon GP, Pappenberger F, Van Dijk AI, et al. Daily evaluation of 26 precipitation datasets using Stage-IV gauge-radar data for the CONUS. Hydrol Earth Syst Sci. 2019;23(1):207–24. https://doi.org/10.5194/hess-23-207-2019

40. Amarjyothi K, Kumar DP, Reddy MV, Mitra AK, Sreevathsa MR, Neha Rajput M, et al. How well do multi-source ensemble rainfall products capture precipitation during monsoons in India? Meteorol Atmos Phys. 2025;137(6):49. https://doi.org/10.1007/s00703-025-01098-4

41. Derin Y, Anagnostou E, Berne A, Borga M, Boudevillain B, Buytaert W, et al. Multiregional satellite precipitation products evaluation over complex terrain. J Hydrometeorol. 2016;17(6):1817–36. https://doi.org/10.1175/JHM-D-15-0197.1

42. Bai P, Liu X. Evaluation of five satellite-based precipitation products in two gauge-scarce basins on the Tibetan Plateau. Remote Sens. 2018;10(8):1316. https://doi.org/10.3390/rs10081316

43. Kumar P, Mishra AK, Dubey AK, Javed A, Saharwardi MS, Kumari A, et al. Regional earth system modelling framework for CORDEX-SA: an integrated model assessment for Indian summer monsoon rainfall. Clim Dyn. 2022;59(7):2409–28. https://doi.org/10.1007/s00382-022-06217-0

44. Xiang Y, Chen J, Li L, Peng T, Yin Z. Evaluation of eight global precipitation datasets in hydrological modeling. Remote Sens. 2021;13(14):2831. https://doi.org/10.3390/rs13142831

45. Pazhanivelan S, Geethalakshmi V, Samykannu V, Kumaraperumal R, Kancheti M, Kaliaperumal R, et al. Evaluation of SPI and rainfall departure based on multi-satellite precipitation products for meteorological drought monitoring in Tamil Nadu. Water. 2023;15(7):1435. https://doi.org/10.3390/w15071435

46. Kumar V, Borgemeister C, Tischbein B, Kumar N. Evaluation and inter-comparison of twenty-three gridded rainfall products representing a typical urban monsoon climate in India. Theor Appl Climatol. 2024;155(11):9529–53. https://doi.org/10.1007/s00704-024-05191-3

Additional information

Peer review: Publisher thanks the Sectional Editor and anonymous reviewers for their contribution to the peer review of this work.

Reprints & permissions information: Available at https://horizonepublishing.com/journals/index.php/PST/open_access_policy.

Publisher's Note: Horizon e-Publishing Group remains neutral with regard to jurisdictional claims in published maps and institutional affiliations.

Indexing: See https://horizonepublishing.com/journals/index.php/PST/indexing_abstracting.

Copyright: © The Author(s). This is an open-access article distributed under the Creative Commons Attribution License CC BY 4.0.

Publisher information: Plant Science Today is published by Horizon e-Publishing Group with support from Empirion Publishers Private Limited, Thiruvananthapuram, India.

© The Author(s) 2026. Creative Commons CC BY 4.0. Published by Horizon e-Publishing Group.

https://doi.org/10.14719/pst.16504